General Disclaimer

One or more of the Following Statements may affect this Document

- This document has been reproduced from the best copy furnished by the organizational source. It is being released in the interest of making available as much information as possible.

- This document may contain data, which exceeds the sheet parameters. It was furnished in this condition by the organizational source and is the best copy available.

- This document may contain tone-on-tone or color graphs, charts and/or pictures, which have been reproduced in black and white.

- This document is paginated as submitted by the original source.

- Portions of this document are not fully legible due to the historical nature of some of the material. However, it is the best reproduction available from the original submission.

THE INFLUENCE OF TEMPERATURE ON FATIGUE-CRACK GROWTH IN A MILL-ANNEALED Ti-6Al-4V ALLOY

by

R. P. Wei* and D. L. Ritter**
LEHIGH UNIVERSITY
Bethlehem, Pennsylvania

NAL - 39 - 007 - 040

ABSTRACT

To understand the influence of temperature on the rate of fatigue-crack growth in high-strength metal alloys, constant-load-amplitude fatigue-crack growth experiments were carried out using a $\frac{1}{4}$-inch-thick (6.35 mm) mill-annealed Ti-6Al-4V alloy plate as a model material. The rates of fatigue-crack growth were determined as a function of temperature, ranging from room temperature to about 290 C (or, about 550 F/563K) and as a function of the crack-tip stress-intensity factor ΔK, in a dehumidified high-purity argon environment. The results indicate that the rate of fatigue-crack growth for ΔK from 10 ksi $\sqrt{in.}$ to 30 ksi $\sqrt{in.}$ (11 to 33 MN-m$^{-3/2}$), corresponding to growth rates from 2×10^{-7} to 4×10^{-4} inch per cycle (5.08×10^{-6} to 1.16×10^{-2} mm/cycle) are essentially independent of test temperature in this range. The dependence of the rate of fatigue-crack growth on ΔK appears to be separable into two regions, with a transition occuring in the range of 2 to 3×10^{-6} inch per cycle (5.08 to 7.62×10^{-5} mm/cycle). The transition correlates well with changes in both the microscopic and macroscopic appearances of the fracture surfaces, and suggests a change in the mechanism and the influence of microstructure on fatigue-crack growth.

Limited correlative experiments indicate that dehumidified oxygen and hydrogen have no effect on the rate of fatigue-crack growth in this alloy, while distilled water increased the rate of crack growth slightly in the range tested. Crack growth in vacuum (less than 5×10^{-6} torr) was about one-half that observed in the dehumidified argon environment. Mass spectrometric analysis and other experiments suggest that this difference is produced by residual moisture (well below 30 ppm) in the argon atmosphere. The possible influence of this residual moisture on the observed temperature independence is discussed.

Companion fractographic examinations suggest that the mechanisms for fatigue-crack growth in the various environments are essentially the same. The observation of ductile striations on specimens tested in vacuum (4.4×10^{-7} to 2.9×10^{-9} torr) is not in agreement with previous investigations on aluminum alloys. Possible reasons for this discrepancy are discussed.

---

* Professor, Department of Mechanical Engineering and Mechanics.

** Assistant Professor, Department of Metallurgy and Materials Science.

I. INTRODUCTION

The importance of fatigue-crack growth resistance in determining the serviceable lives of aircraft structures has been well recognized [1]*. With the development of aircrafts to operate at flight speeds in excess of the speed of sound, such as the supersonic transport (SST), the fatigue-crack growth resistance of materials over a wide range of temperatures, associated with aerodynamic heating, needs to be considered. Recent investigations have shown that atmospheric moisture and other environments (such as water, salt water, salt and certain organic liquids) can also have a significant effect on the rate of fatigue-crack growth in high-strength alloys [2-16] and that these environmental influences are affected by temperature [10]. Thus, the performance of structures in service will depend on the complex interactions between loads, temperatures and environments encountered during the entire flight profile.

Fatigue-crack growth resistance of candidate materials for the United States Supersonic Transport at room temperature and at 550F (or, about 290C/563K) has been evaluated by C. M. Hudson at the NASA Langley Research Center [17]. For some of the materials, fatigue-crack growth resistance at -109F (or, about -78C/195K) was also determined [17]. No consistent pattern of behavior with temperature was evident. Since these tests were conducted in air, the results may reflect the combined influences of atmospheric moisture and temperature [10, 11]. In a recent series of experiments, the effect of temperature on the rate of fatigue-crack growth in a 7075-T651 aluminum alloy was examined over a range of temperatures from room temperature to approximately 100C (373K/212F) in distilled water and in dehumidified hydrogen and oxygen environments. Dehumidified high-purity argon (99.9995 percent purity) was used as a reference

* See References.

environment. The results show that fatigue-crack growth is controlled by thermally activated processes with apparent activation energies that depend strongly on the crack-tip stress-intensity factor, ΔK or K, given by linear elasticity for all of the test environments [10, 11]. The strong effect of ΔK on the apparent activation energy for crack growth implies that the influence of temperature on the rate of fatigue-crack growth will be a function of ΔK; the effect of temperature being stronger at the lower ΔK levels [10, 11]. These findings suggest that the effect of temperature might be incorporated explicitly in design through an absolute rate theory consideration of the fatigue-crack growth process. Verification of the general applicability of this concept and further quantitative development of this approach would be of both technological and fundamental importance.

Since only a limited amount of information of this type is available, an experimental program was initiated to determine the rate of fatigue-crack growth on a single high-strength alloy over a wide range of temperatures and crack growth rates. The experiments were carried out principally in a dehumidified high-purity argon atmosphere to "eliminate" the interaction effects of aggressive environments. The results are intended for use in verifying and guiding development of analytical methods for estimating fatigue-crack growth that would incorporate temperature dependence explicitly. Because of its importance in SST applications, annealed Ti-6Al-4V alloy was selected as model material for this study. Test temperature ranging from room temperature to about 290C (or about 563K/550F) were used. Companion fractographic examinations of selected specimens were made to determine possible changes in crack morphology (or cracking mechanism) with changes in test temperature and environment.

The fatigue-crack growth and the fractographic studies will be discussed separately.

II. THE KINETICS OF CRACK GROWTH

MATERIAL AND EXPERIMENTAL WORK

Material and Specimens

Two ¼-inch-thick (6.35 mm) plates of mill-annealed Ti-6Al-4V alloy were furnished from NASA Langley Research Center stock for this investigation. The dimensions of the plates were 36 inches (914 mm) wide by 43 inches (1090 mm) long and 12 inches (305 mm) wide by 24 inches (610 mm) long. These plates were cut from a single plate of material (Heat No. D-4987) and conforms to AMS 4911 specification. The nominal chemical composition of this material is given in Table 1. Longitudinal and transverse tensile-test specimens and 3-inch-wide (76.2 mm) by 12-inch-long (305 mm) single-edge notch (SEN) fracture-test specimens were prepared in triplicate and tested (see Figure 1 for specimen layout). The tensile properties and crack growth resistance curves (for monotonic loading) are shown in Table 1 and Figure 2 respectively, and are typical of this alloy in the mill-annealed condition. These results suggest that these plates were cross rolled, with a cross rolling ratio of nearly 1:1. On the basis of these results, these plates were judged to be typical of mill-annealed Ti-6Al-4V alloy and were suitable for use in this program. Optical micrographs show representative α-β structure for this alloy, Figure 3.

Three-inch-wide (76.2 mm) by 14-inch-long (356 mm) center-cracked specimens, oriented in the LT (or RW) orientation,* were used for the fatigue-crack growth studies (see Figure 1 for plate layout). The initial center notch, about 0.4 inch (about 10 mm) long, was introduced by broaching. The specimens were precracked in air, or in

"ultra-high-purity" grade argon (99.999 percent purity) at a stress ratio R of 0.05 through a sequence of loads that reduce ΔK to a level that is equal to or less than the selected starting ΔK level for the actual experiment. This precracking procedure provided fatigue-cracks of about 0.08 inch (2 mm) in length from the ends of the starter notches, such that subsequent fatigue-crack growth will be through material that has not been altered by the notch preparation procedure and will be unaffected by the starter notch geometry.

Test Environment

Dehumidified Matheson "Research" grade argon (99.9995 percent purity) was used as the principal test environment. Dehumidified Matheson "Ultra-Pure" grade oxygen (99.95 percent purity) and hydrogen (99.999 percent purity) and distilled water were also used to provide supplemental information. The dehumidified gaseous environments were obtained by passing the respective gases through a gas purifier (Matheson Model 460 purifier with Model 461-R cartridge for moisture), then through a series of cold traps at less than -140C (~130K), and finally through a silicone fluid back-diffusion trap and discharged. The gas dehumidification train is illustrated schematically in Figure 4.

---

* ASTM Committee E-24 on Fracture Testing of Metals has adopted the following convention to denote the plane and direction of cracking [18]. The first letter, in the two letter coding, denotes the direction normal (perpendicular) to the macroscopic crack plane, while the second denotes the direction of crack growth. R, W and T have been used to denote the rolling (longitudinal), width (transverse) and thickness (short transverse) directions respectively. To provide greater consistency and clarity, Committee E-24 will adopt the designations L, T and S, respectively, for these three principal directions in rolled plate product. The new designations are used in this report. For clarity, the old designations are also included parenthetically.

Distilled water used in the experiments was triple-distilled water purchased commercially.

Because of the highly reactive nature of the titanium alloys, limited correlative experiments were conducted with C. M. Hudson of NASA Langley Research Center to compare test results obtained in dehumidified high-purity argon with those obtained in vacuum at 2-5 x 10^{-7} torr.

Experimental Procedures

The fatigue-crack growth experiments were carried out under axial loading at R = 0.05 in an 100,000-lb. capacity MTS Systems closed-loop electro-hydraulic testing machine operated at either 5 or 10 Hz.* (300 or 600 cycles per minute). Load control was estimated to be better than ±1 percent. After precracking the specimen, appropriate environmental chambers were clamped in place [7]. For tests in distilled water, cup-type chambers were used. These were simply filled with distilled water. Testing was started after a short period for instrument stablization. For the dehumidified gaseous environments, a rigorous purging procedure was followed. The gas train was purged with "Ultra-High-Purity" grade argon for at least 30 minutes. During this initial purging operation, the various components of the gas train up-stream from the back-diffusion trap (Figure 4) were heated to at least 100C (373K). The cold-traps were then filled with liquid nitrogen, and the environment chamber-specimen assembly was again heated to a minimum of 100C (373K) while maintaining the argon flow.** The specimen

---

* Comparison experiments indicated that test frequencies from 1 to 15 Hz. had negligible effect on the rate of fatigue-crack in this material tested in a dehumidified argon environment.

** This step was combined with specimen heating whenever the test temperature was to exceed 100C (373K).

was then brought to the desired test temperature by means of electrical resistance heating tapes. (Temperature stability was better than ± 2C during a working day.) Appropriate test environment was introduced and was allowed to flow through the system for at least 15 minutes prior to the start of the experiment. Continuous flow at a chamber pressure of about 5 psi (35 kN/m^2) above ambient was maintained throughout the experiment.

A continuous-recording electrical potential system was used for monitoring crack growth, Figure 5. The detailed experimental procedure and calibration of this method have been described elsewhere [19, 20]. Using a working current of 2.5 amperes, this system provides an average measurement sensitivity of about 0.003 inch (0.076 mm) in half-crack length (a) per microvolt (μv) change in potential, (0.003 in./μv or 0.076 mm/μv), for the $\frac{1}{4}$-inch-thick (6.35 mm) Ti-6Al-4V alloy specimens. The variation of measurement sensitivity with crack length for a typical specimen is shown in Figure 6; the actual sensitivity varies somewhat with the thickness of each specimen. Resolution is better than 0.0015 inch (0.038 mm) in half-crack length, a. For comparison, both the electrical potential method and a visual method, using a photogrid technique [17] were used to monitor crack growth on a single specimen. The results of this study are shown in Figure 7 and show the good agreement between these two methods. (Note that corrections for crack front curvature were needed in making this comparison, since the visual method measures the crack lengths at the specimen surface whereas the electrical potential method provides an average through the specimen thickness).

RESULTS AND DISCUSSIONS

Fatigue-Crack Growth Results

Fatigue-Crack growth rate data were determined from the slopes of the electrical potential records and correlated with the crack-tip stress-intensity parameter ΔK.

$$\Delta K = \Delta \sigma \sqrt{\pi a} \cdot f(a/W) \qquad (1)$$

where $\Delta \sigma$ = range of applied gross-section stress

a = half-crack length

$f(a/W)$ = correction factor for finite-width specimen [21, 22]

W = specimen width

Data for tests conducted in dehumidified argon at temperatures from room temperature to about 290C (or about 70 to 550F/300 to 563K) are shown in Figures 8 to 13, and are also tabulated as crack-length (a) versus number of elapsed load cycles (N) in Table 2. These results covered a range of stress-intensity parameters (ΔK) from about 10 to 35 ksi $\sqrt{in.}$ (11 to 38.5 MN-$m^{-3/2}$) with corresponding crack growth rates ($\Delta a/\Delta N$) from about 2×10^{-7} to 5×10^{-4} inch per cycle (5.08×10^{-6} to 1.27×10^{-2} mm/cycle). Reproducibility was generally within $\pm$ 10 percent. Larger variations at the lower growth rates were principally caused by drift in the crack length monitoring system, associated with small changes in specimen temperature, and possible delay produced by the precracking procedure [24]. The growth rates for selected values of ΔK, at the various temperatures, are shown in a standard Arrhenius plot in Figure 14. It is seen that the rates of fatigue-crack growth, for ΔK from 10 to 30 ksi $\sqrt{in.}$ (11 to 33 MN-$m^{-3/2}$ are essentially independent of temperature in the range of 20 to 290C (or, about 70 to 550F/300 to 563K), in contradistinction to that of the 7075-T651 aluminum alloy [10]. The dependence of the

rate of fatigue-crack growth on Δ K appears to be separable into two regions, with a transition occurring in the range of 2 to 3 x 10^{-6} inch per cycle (5.08 to 7.63 x 10^{-5} mm/cycle), as shown typically in Figure 8. Using a piece-wise power-law [23] fit to the experimental data, that is

$$\frac{\Delta a}{\Delta N} = C(\Delta K)^n \qquad (2)$$

the exponent n is the range of 7 to 10 for growth rates ($\Delta a/\Delta N$) between 2 x 10^{-7} and 2 x 10^{-6} inch per cycle (5.08 x 10^{-6} to 5.08 x 10^{-5} mm/cycle), and is about 3 in the range 2 x 10^{-6} to 5 x 10^{-4} inch per cycle (5.08 x 10^{-5} to 1.27 x 10^{-2} mm/cycle), Figures 8 to 13. This transition suggests a change in the mechanism of fatigue-crack growth and correlates well with a change in the macroscopic appearance of the fracture surface, Figure 15. The fracture is quite coarse (macroscopically) at growth rates below the transition range of 2 to 3 x 10^{-6} inch per cycle (5.08 to 7.62 x 10^{-5} mm/cycle) and becomes smooth at the higher rates of growth. A more detailed discussion of the changes in fracture mechanism will be given in the fractographic section (Section III) of this report.

To complement these studies, a limited number of experiments were carried out in dehumidified hydrogen and oxygen and in distilled water to examine the effects of these environments on the rate of fatigue-crack growth, and a correlative study was conducted in cooperation with C. M. Hudson of NASA Langley Research Center to determine if any differences existed between data obtained in dehumidified high-purity argon and those obtained in vacuum at 10^{-6} to 10^{-7} torr. The results of these studies are shown in Figures 16 to 21. An additional test was carried out at -61C (-78F/212K) and 2.9 x 10^{-9} torr; the results of this test are shown in Figure 22. Crack length versus number of elapsed load cycle information for these tests are tabulated in Tables 3

to 6. It is seen that data obtained in dehumidified oxygen (Figures 16 and 17) and hydrogen (Figure 18) are nearly identical to those for dehumidified argon for ΔK ranging from about 15 to 30 ksi/in. (16.5 to 33 MN-$m^{-3/2}$). For the same range of ΔK, distilled water increased the rate of fatigue-crack growth by about 50 percent at low ΔK levels, whereas at the higher ΔK levels the rate of growth approached that for dehumidified argon, Figures 19 and 20. The results suggest that the rate of fatigue-crack growth in these environments are again independent of temperature.

Data obtained in vacuum (2.1×10^{-7} and 4.4×10^{-7} torr) at room temperature are some 30 to 50 percent slower than those obtained in dehumidified argon at low ΔK levels and tended to converge with the dehumidified argon results at the higher ΔK levels, Figure 21. Careful rechecking of testing machine calibration and experimental procedures, both at Lehigh University and at NASA Langley, and additional comparative experiments using distilled water from a single source as the test environment, Figure 21, suggest that these differences are real and significant;(the interlaboratory reproducibility being approximately 10 percent). On the basis of these experiments, a mass spectrometric analysis of the dehumidified argon atmosphere was initiated, and further purification of the gases was attempted (see following discussions). Test results at -61C (-78F/212K) were essentially the same as those obtained at room temperature, and suggest that the temperature independence may be extended to this low temperature.

Mass Spectrometric Analysis Results

A sample for mass spectrometric analysis was collected by inserting a collection bulb just down-stream of the environment chamber. The standard purging procedure was used with the exception that the system was evacuated with a mechanical pump and back-filled with argon several times before the regular purging sequence to ensure

removal of air from the collection bulb. The sample was analyzed in a Hitachi mass spectrometer*. The results indicate that the amount of nitrogen and oxygen in the dehumidified argon sample was less than 30 and 8 ppm (parts per million) respectively. These contaminants may be introduced by the sample collection procedure (i.e., from air trapped in the stop-cocks), during transfer into the mass spectrometer, or by possible leakage in the environmental system. The determination of moisture level was much more uncertain. The amount of moisture present could not be resolved from the background moisture level in the instrument. Based on the sensitivity limits of the instrument, it was estimated that the moisture content was well below 30 ppm.

Concurrent with this examination, attempts to further purify the test environment were made. It was found that by using a titanium sublimation pump as a getter in the argon stream, reduction in the rate of fatigue-crack growth (comparable to the percentage difference between vacuum and dehumidified argon results), was obtained on another mill-annealed Ti-6Al-4V alloy plate.

On the basis of these results, it is clear that residual impurities at levels below 30 ppm can still affect fatigue-crack growth in this titanium alloy. Since the influence of oxygen at $\sim$1 atmosphere (Figures 16 and 17) did not significantly increase the rate of fatigue-crack growth, the active impurity is considered to be moisture (water vapor) present in the argon atmosphere.

Discussion

The absence of temperature dependence for the rate of fatigue-crack growth in the mill-annealed Ti-6Al-4V alloy in the range of 2×10^{-7} to 5×10^{-4} inch per cycles

---

* Analysis performed by Dr. J. Sturm, Department of Chemistry, Lehigh University.

(5.08×10^{-6} to 1.27×10^{-2} mm/cycle) should be interpreted with care. Although the results are in general agreement with that reported by Hudson [17] for a Ti-8Al-1V-1Mo alloy, the apparent sensitivity of this titanium alloy to residual moisture of less than 30 ppm did not permit a clear resolution of the problem that the influence of temperature associated with deformation may have been compensated by that resulting from environmental embrittlement in a partially saturated environment [10, 25]. If one can assume that the effect of environment has a decreasing branch with temperature as indicated by Johnson and Willner [25] for environments containing a fixed amount of moisture, then the fatigue-crack growth in a truly inert environment may be shown to be dependent on temperature. This particular point still needs to be investigated.

The apparent lack of temperature dependence in the range of growth rates from 2×10^{-7} to 5×10^{-4} inch per cycle (5.08×10^{-6} to 1.27×10^{-2} mm/cycle) does not imply complete temperature independence over the entire range of growth rates. For growth rates in excess of about 10^{-4} inch per cycle (2.5×10^{-3} mm/cycle), crack growth approaches the onset of rapid fracture or fracture instability, and is expected to be related to the fracture toughness of the material, K_{Ic} or K_c. Since fracture toughness is known to be dependent on temperature, some influence of temperature on the rate of fatigue-crack growth at these high rates would be expected. It is interesting to note that, by comparing Figures 2 and 11, the value of K_{max} ($K_{max} = \Delta K/(1-R)$) for transition to rapid fatigue-crack growth (i.e. $\Delta a/\Delta N > 10^{-4}$ in/cycle or 2.5×10^{-3} mm/cycle) corresponds to the K level for the onset of crack growth under monotonic loading.

Practically, the observed temperature independence permits a degree of simplification in estimating the fatigue performance of structures intended for service at various temperatures. However, the possible interactions between temperature and load under

conditions of changing loads and temperatures encountered during service may be quite significant and must be carefully explored. This problem is being investigated currently.

III. FRACTOGRAPHY

MATERIAL AND EXPERIMENTAL WORK

Selected specimens, tested in the various environments and at different temperatures were examined by means of optical microscopy and electron-microfractography to determine possible changes in crack morphology, or cracking mechanism, and the relationship between crack paths and microstructure.

For electron-microfractography, two-stage plastic-carbon replicas shadowed with platinum-carbon were used. The shadowing direction was along the direction of crack prolongation. Replicas were taken from regions of the fracture surface corresponding to observed macroscopic crack growth rates of 1 to 3 x 10^{-5} inch per cycle (2.54 to 7.62 x 10^{-4} mm/cycle), and to those above and below the observed macroscopic transition region, 2 to 3 x 10^{-6} inch per cycle (5.08 to 7.62 x 10^{-5} mm/cycle), Figure 8 to 13 and 15. They were examined in a RCA EMU-3G electron microscope operated at 50 or 100 kV. Specimen tilting was used to enhance contrast [26]; tilt angles up to 30° were used.

In pertinent cases, specimens were plated with nickel and then sectioned to examine the interaction of the propagating crack with the alloy microstructure by optical microscopy.

RESULTS AND DISCUSSIONS

Effects of Environment and Temperature

Typical electron-micrographs of fatigue fracture surfaces of specimens tested in the various environments and temperatures are shown in Figure 23. The results indicate that there are no significant differences in the failure mode and fracture paths for specimens tested at different temperatures and in the different environments, with ductile

fatigue striations as the predominant feature in all cases. The striation spacings correspond, within expected accuracy, to the observed macroscopic crack growth rate of about 2×10^{-5} inch per cycle (5×10^{-4} mm/cycle). These observations are consistent with the fact that there were no significant influence of test environment and temperature on the rate of fatigue-crack growth for this alloy.

The observation of ductile striations on specimens of Ti-6Al-4V alloy tested in vacuum (at 4.4×10^{-7} to 2.9×10^{-9} torr) is not in agreement with the results reported by Pelloux [27] and Meyn [28] for aluminum alloys. These workers suggested that the mechanism for fatigue-crack growth is different from that in air, and therefore, should not lead to striation formation. Two probable reasons can be cited to account for the apparent discrepancy, aside from the fact that different alloys are involved. Both reasons are related to the ability to clearly resolve striations by replication electron microscopy. First, the striations in specimens tested in vacuum have a flattened and smeared appearance, Figure 23(c & d), and hence, would be more difficult to resolve. Broek showed that by tilting the replica with respect to the electron beam, enhanced contrast may be obtained [26]; regions that appeared relatively "featureless" under one set of viewing conditions were shown to contain fatigue striations and other structural features. This technique was utilized to examine replicas from specimens tested in vacuum. The results indeed demonstrate that, under certain orientations, regions that contain striations can be made to appear nearly featureless, Figures 24 and 25. The second possibility is that the rate of fatigue-crack growth, and hence, the striation spacing, could be well below the resolution limits of replication electron-microscopy technique [29]; the limit has been variously estimated at some 200 to 500 Å. This may well be the case for the work on aluminum alloys reported by Pelloux [27]

and Meyn [28]. Since these alloys are known to be quite sensitive to the effect of atmospheric moisture, an order of magnitude reduction in crack growth rate associated with a change in test environment, from air to vacuum, is possible. The striations, if present, at the reduced rates of growth may not have been resolvable. Regardless, it is clear that the mechanisms for fatigue-crack growth in the Ti-6Al-4V alloy are essentially the same for all the environments investigated.

Low Growth Rates

For specimens tested at low ΔK levels, corresponding to growth rates below about 2×10^{-6} inch per cycle (5×10^{-5} mm/cycle), a macroscopically observable coarse region of crack growth was observed (see Figure 15). Above approximately 2×10^{-6} inch per cycle (5×10^{-5} mm/cycle), the macroscopic texture of the fracture surfaces appeared to be fine. This change in fracture appearance corresponds to the transition in the crack-growth-rate versus ΔK curves, Figures 8 to 13, and suggests a change in the mechanism for fatigue-crack growth. (By alternating between "high" and "low" ΔK's to produce crack-growth-rates above and below the transition range of 2 to 3×10^{-6} inch per cycle (5.08 to 7.62×10^{-5} mm/cycle), alternate fine and coarse regions of crack growth may be produced.)

Typical electron-micrographs of fatigue-crack surfaces in the fine and coarse regions are shown in Figure 26. In the "fine" region, ductile fatigue striations predominate, Figure 26(a); while in the "coarse" region a more irregular fracture surface with regions of "quasi-cleavage" are observed, Figure 26(b). Optical microscopy results (on sections parallel to the plate surface) show extensive crack branching in the coarse region, and indicate progression of cracks from one second-phase particle

to another, and occasional fracturing of the second-phase particles (Figures 27 and 28). No detailed mechanism for crack growth can be determined or postulated. Although no striations were observed, a mechanism of crack growth associated with ductile fatigue striation formation could not be ruled out, since at these low rates of growth individual striations (with spacings less than 500 Å) would not be resolvable with the current plastic-carbon replication techniques.

SUMMARY

Constant-load-amplitude fatigue-crack growth experiments were carried out on a ¼-inch-thick (6.35 mm) mill-annealed Ti-6Al-4V alloy plate in dehumidified argon to study the effects of temperature and crack driving force, characterized by the crack-tip stress intensity factor ΔK, on crack growth. A range of temperature from room temperature to about 290C (or, 563K/550F) were investigated. The results indicate that the rate of fatigue-crack growth, for ΔK from 10 ksi $\sqrt{in.}$ to 30 ksi $\sqrt{in.}$ (11 to 33 MN-$m^{-3/2}$), corresponding to growth rates from 2×10^{-7} to 4×10^{-4} inch per cycle (5.08×10^{-6} to 1.16×10^{-2} mm/cycle) were essentially unaffected by temperature in this range. The dependence of the rate of fatigue-crack growth on ΔK appears to be separable into two regions, with a transition occurring in the range of 2 to 3×10^{-6} inch per cycle (5.08 to 7.62×10^{-5} mm/cycle). The transition correlates well with changes in both the macroscopic and microscopic appearances of fracture surfaces, and suggests a change in the mechanism and the influence of microstructure on fatigue-crack growth.

Limited correlative experiments indicate that dehumidified oxygen and hydrogen had no effect on the rate of fatigue-crack growth in this alloy, while distilled water increased the rate of crack growth by 30 to 50 percent for ΔK from 15 to 30 ksi $\sqrt{in.}$ (17.5 to 33 MN-$m^{-3/2}$). Crack growth in vacuum, at less than 5×10^{-6} torr, was about one-half that observed in the dehumidified gaseous environments for the same range of ΔK. Mass spectrometric analysis and other experiments suggest that residual moisture, well below 30 ppm, can have a deleterious effect on this alloy. The observed temperature independence may still be caused by the compensating influences of moisture and deformation on fatigue-crack growth, and should be investigated further.

Companion fractographic sutdies showed that the mechanisms for fatigue-crack growth in the various environments, including vacuum, are essentially the same. The observation of ductile striations on specimens tested in vacuum is not in agreement with previous investigations on aluminum alloys. This discrepancy is believed to be caused principally by problems of contrast and resolution in the replication electron-microfractography technique.

Although the apparent temperature independence provides a degree of simplification in estimating the service performance of structure, the interactions between load and temperature under conditions of changing loads and temperatures encountered during service may be quite significant and should be carefully explored.

ACKNOWLEDGMENT

The authors wish to express their appreciation to Mr. C. M. Hudson for carrying out the experiments in vacuum at NASA Langley; to Dr. J. Sturm for performing the mass spectrometric analysis; to Mr. J. H. FitzGerald for his careful experimental work; to Mr. R. Korastinsky for electron-microfractography; and to Messrs. E. Herrold and T. T. Shih for their assistance in data reduction.

REFERENCES

1. Hardrath, H. F. "Fatigue and Fracture Mechanics," AIAA Paper No. 70-512, April 1970.

2. Hartman, A. "On the Effect of Oxygen and Water Vapor on the Propagation of Fatigue Cracks in 2024-T3 Al Clad Sheet," International Journal of Fracture Mechanics, Vol. 1, 1965, pp. 167-188.

3. Bradshaw, F. J. and Wheeler, C. "The Effect of Environment on Fatigue-Crack Growth in Aluminum and Some Aluminum Alloys," Applied Materials Research, Vol. 5, 1966, pp. 112-120.

4. Judy, R. W., Crooker, J. W., Morey, R. E., Lange, E. A., and Goode, R. J. "Low-Cycle Fatigue-Crack Propagation and Fractographic Investigation of Ti-7Al-2Cb-1Ta and Ti-6Al-4V in Air and in Aqueous Environments," ASM Transactions, Vol. 59, 1966, pp. 195-207.

5. Dahlberg, E. P., "Fatigue-Crack Propagation in High-Strength 4340 Steel in Humid Air," ASM Transactions, Vol. 58, 1965, pp. 46-53.

6. Li, Che-Yu, Talda, P. M., and Wei, R. P. "The Effect of Environments on Fatigue-Crack Propagation in an Ultra-High-Strength Steel," International Journal of Fracture Mechanics, Vol. 3, No. 1, 1967, pp. 29-36.

7. Wei, R. P., Talda, P. M., and Li, Che-Yu "Fatigue-Crack Propagation in Some Ultra-High-Strength Steels," ASTM STP 415, 1967, pp. 460-485.

8. Spitzig, W. A., Talda, P. M., and Wei, R. P. "Fatigue-Crack Propagation and Fractographic Analysis of 18Ni (250) Maraging Steel Tested in Argon and Hydrogen Environments," Journal of Engineering Fracture Mechanics, Vol. 1, No. 1, 1968, pp. 155-166.

9. Achter, M. R. "Effect of Environment on Fatigue Cracks," ASTM STP 415, 1967, pp. 181-204.

10. Wei, R. P. "Fatigue-Crack Propagation in a High-Strength Aluminum Alloys," International Journal of Fracture Mechanics, Vol. 4, No. 2, 1968, pp. 159-170.

11. Wei, R. P. "Some Aspects of Environment-Enhanced Fatigue-Crack Growth," Journal of Engineering Fracture Mechanics, Vol. 1, No. 4, 1970, pp. 633-652.

12. Feeney, J. A., McMillan, J. C. and Wei, R. P. "Environmental Fatigue Crack Propagation of Aluminum Alloys at Low Stress Intensity Levels," Metallurgical Transactions, Vol. 1, 1970, pp. 1741-1757.

13. Hartman, A. and Schijve, J. "The Effects of Environment and Load Frequency on the Crack Propagation Law for Macro Fatigue Crack Growth in Aluminum Alloys," International Journal of Fracture Mechanics, Vol. 1, No. 4, 1970, pp. 615-632.

14. Landes, J. D. "Kinetics of Subcritical-Crack Growth and Deformation in a High-Strength Steel," Ph. D. dissertation, Lehigh University, 1970.

15. Wei, R. P. and Landes, J. D. "Correlation between Sustained-Load and Fatigue Crack Growth in High-Strength Steels," Materials Research and Standards, ASTM, Vol. 9, No. 7, 1969, p. 25.

16. Bucci, R. "Environment Enhanced Fatigue and Stress Corrosion Cracking of a Titanium Plus a Simple Superposition Model for Assessment of Environmental Influence on Fatigue Behavior," Ph. D. dissertation, Lehigh University, 1970.

17. Hudson, C. M. "Fatigue-Crack Propagation in Several Titanium and Stainless-Steel Alloys and One Superalloy," NASA TN-D-2331, October 1964.

18. Anonymous, "The Slow Growth and Rapid Propagation of Cracks," Materials Research and Standards, ASTM, Vol. 1, 1961, p. 389.

19. Johnson, H. H. "Calibrating the Electric Potential Method for Studying Slow Crack Growth," Materials Research and Standards, ASTM, Vol. 5, No. 9, 1965, p. 442.

20. Li, Che-Yu and Wei, R. P. "Calibrating the Electrical Potential Method for Studying Slow Crack Growth," Materials Research and Standards, Vol. 6, No. 8, 1966, p. 392.

21. Isida, M. and Itagaki, Y. "Stress Concentration at the Tip of a Transverse Crack in a Stiffened Plate Subjected to Tension," Proceedings, 4th U.S. Congress of Applied Mechanics, Berkeley, Calif., 1962.

22. Federson, C.E., Discussion, ASTM STP 410, 1967, pp. 77-79.

23. Paris, P. C. and Erdogan, F. "A Critical Analysis of Crack Propagation Laws," Journal of Basic Engineering, ASME, December 1963.

24. Jonas, O. and Wei, R. P. "An Exploratory Study of Delay in Fatigue-Crack Growth," International Journal of Fracture Mechanics, 1971 (to be published).

25. Johnson, H. H. and Wilmer, A. M. "Moisture and Stable Crack Growth in a High Strength Steel," Applied Materials Research, Vol. 4, 1965, p. 34.

26. Broek, D. "A Critical Note on Electron Fractography," Journal of Engineering Fracture Mechanics, Vol. 1, No. 4, 1970, pp. 691-696.

27. Pelloux, R. M. N. "Crack Extension by Alternating Shear," Journal of Engineering Fracture Mechanics," Vol. 1, No. 4, 1970, pp. 697-704.

28. Meyn, D. "The Nature of Fatigue Crack Propagation in Air and in Vacuum for 2024 Aluminum," Transactions ASM, Vol. 61, No. 1, 1968.

29. Whiteson, B. V. et al, "Electron Fractography Handbook," Technical Report ML TDR-64-416, Air Force Materials Laboratory, Wright-Patterson Air Force Base, Ohio.

TABLE 1

CHEMICAL COMPOSITION AND TENSILE PROPERTIES OF MATERIAL INVESTIGATED

Nominal Chemical Composition (weight percent)

C	Al	V	Fe	N	H	O	Ti
0.10 max.	5.50 to 6.75	3.50 to 4.50	0.30 max.	0.05 max.	0.015 max.	0.20 max.	Balance

Tensile Properties

Specimen No. and Direction	0.2% Offset Yield Strength ksi (MN/m^2)	Tensile Strength ksi (MN/m^2)	Elongation in 2 in. percent
Longitudinal			
T1-37L	136.4 (941)	144.3 (995)	14.0
T1-38L	140.8 (971)	147.1 (1015)	14.0
T1-39L	140.2 (967)	146.1 (1008)	14.0
(Average)	139.1 (959)	145.8 (1006)	14.0
Transverse			
T1-40T	139.9 (965)	144.8 (999)	14.0
T1-41T	140.9 (972)	144.8 (999)	14.5
T1-42T	143.0 (986)	146.1 (1008)	14.0
(Average)	141.3 (974)	145.2 (1002)	14.2

Table 2: Fatigue-Crack Growth in Dehumidified Argon at Various Test Temperatures

SPECIMEN TI 24 ENVIRON. ARGON WIDTH = 3.000 IN. THICK. = .241 IN. TEMP. = 22.00 C
MAXIMUM LOAD =10.00 KIPS STRESS RATIO = .050 FREQUENCY = 5.0 HZ NO. OF POINTS = 26

CRACK LENGTH (1)	NO. OF CYCLES (2)	CRACK LENGTH	NO. OF CYCLES	CRACK LENGTH	NO. OF CYCLES	CRACK LENGTH	NO. OF CYCLES
.351	4.10000E+03	.590	4.57375E+04	.775	5.96525E+04		
.355	7.25000E+03	.605	4.71250E+04	.787	6.02525E+04		
.367	1.02500E+04	.618	4.84375E+04				
.379	1.31000E+04	.632	4.96750E+04				
.389	1.56500E+04	.658	5.19625E+04				
.421	2.22250E+04	.671	5.28625E+04				
.441	2.57500E+04	.684	5.38375E+04				
.460	2.88250E+04	.696	5.46625E+04				
.478	3.16000E+04	.716	5.63325E+04				
.512	3.66250E+04	.731	5.70725E+04				
.529	3.88000E+04	.742	5.77525E+04				
.545	4.06750E+04	.753	5.84125E+04				

SPECIMEN TI 16 ENVIRON. ARGON WIDTH = 3.000 IN. THICK. = .243 IN. TEMP. = 22.50 C
MAXIMUM LOAD =14.00 KIPS STRESS RATIO = .050 FREQUENCY = 5.0 HZ NO. OF POINTS = 31

CRACK LENGTH	NO. OF CYCLES	CRACK LENGTH	NO. OF CYCLES	CRACK LENGTH	NO. OF CYCLES	CRACK LENGTH	NO. OF CYCLES
.277	0.	.495	2.59800E+04	.672	3.41700E+04		
.302	6.60000E+03	.512	2.69925E+04	.685	3.45600E+04		
.315	8.62500E+03	.529	2.79300E+04	.691	3.47500E+04		
.329	1.04250E+04	.545	2.88675E+04	.709	3.52600E+04		
.341	1.20000E+04	.553	2.92800E+04	.721	3.55600E+04		
.353	1.35000E+04	.576	3.04700E+04	.733	3.58400E+04		
.365	1.48500E+04	.591	3.11400E+04	.740	3.59900E+04		
.399	1.83575E+04	.605	3.17500E+04				
.420	2.02425E+04	.619	3.23000E+04				
.440	2.19300E+04	.626	3.25600E+04				
.459	2.34300E+04	.646	3.33200E+04				
.469	2.41050E+04	.659	3.37700E+04				

(1) Half-crack length in center-cracked specimens, in inches.
(2) Calculated from electrical-potential vs. time records. Only three significant figures should be used.

Table 2 (continued)

SPECIMEN TI 29 ENVIRON. ARGON WIDTH = 3.000 IN. THICK. = .245 IN. TEMP. = 24.00 C
MAXIMUM LOAD = 9.00 KIPS STRESS RATIO = .050 FREQUENCY = 5.0 HZ NO. OF POINTS = 26

CRACK LENGTH	NO. OF CYCLES	CRACK LENGTH	NO. OF CYCLES	CRACK LENGTH	NO. OF CYCLES	CRACK LENGTH	NO. OF CYCLES
.313	7.20000E+03	.408	5.37625E+04	.498	7.73875E+04		
.317	1.05000E+04	.415	5.62000E+04	.504	7.85125E+04		
.322	1.35000E+04	.422	5.84500E+04				
.326	1.63500E+04	.429	6.05875E+04				
.335	2.11250E+04	.439	6.35125E+04				
.343	2.63000E+04	.446	6.53500E+04				
.351	3.08000E+04	.452	6.71500E+04				
.360	3.47750E+04	.459	6.87625E+04				
.375	4.16750E+04	.469	7.20250E+04				
.383	4.46750E+04	.474	7.34500E+04				
.390	4.76750E+04	.480	7.48750E+04				
.398	5.01500E+04	.483	7.55125E+04				

SPECIMEN TI 29 ENVIRON. ARGON WIDTH = 3.000 IN. THICK. = .245 IN. TEMP. = 23.00 C
MAXIMUM LOAD = 6.00 KIPS STRESS RATIO = .050 FREQUENCY = 5.0 HZ NO. OF POINTS = 24

CRACK LENGTH	NO. OF CYCLES	CRACK LENGTH	NO. OF CYCLES	CRACK LENGTH	NO. OF CYCLES	CRACK LENGTH	NO. OF CYCLES
.577	5.50000E+03	.648	5.36375E+04				
.579	8.05000E+03	.661	6.05375E+04				
.584	1.39250E+04	.674	6.65375E+04				
.589	1.79000E+04	.687	7.19375E+04				
.599	2.44250E+04	.693	7.44875E+04				
.604	2.78000E+04	.711	8.16125E+04				
.609	3.16250E+04	.723	8.61125E+04				
.613	3.37250E+04	.735	9.03875E+04				
.623	3.93875E+04	.746	9.39875E+04				
.627	4.20500E+04	.752	9.57125E+04				
.632	4.47125E+04	.763	9.91625E+04				
.637	4.71875E+04	.774	1.02612E+05				

Table 2 (continued)

SPECIMEN TI 17 ENVIRON. ARGON WIDTH = 3.000 IN. THICK. = .236 IN. TEMP. = 23.90 C
MAXIMUM LOAD =14.00 KIPS STRESS RATIO = .050 FREQUENCY = 5.0 HZ NO. OF POINTS = 8

CRACK LENGTH	NO. OF CYCLES	CRACK LENGTH	NO. OF CYCLES	CRACK LENGTH	NO. OF CYCLES	CRACK LENGTH	NO. OF CYCLES
.314	3.60000E+03						
.326	4.83750E+03						
.339	6.03750E+03						
.351	7.12500E+03						
.362	8.10000E+03						
.373	9.03750E+03						
.395	1.07250E+04						
.408	1.17000E+04						

SPECIMEN TI 5 ENVIRON. ARGON WIDTH = 3.006 IN. THICK. = .245 IN. TEMP. = 26.20 C
MAXIMUM LOAD =10.00 KIPS STRESS RATIO = .050 FREQUENCY =15.0 HZ NO. OF POINTS = 41

CRACK LENGTH	NO. OF CYCLES	CRACK LENGTH	NO. OF CYCLES	CRACK LENGTH	NO. OF CYCLES	CRACK LENGTH	NO. OF CYCLES
.310	4.40000E+03	.458	3.71375E+04	.628	5.75750E+04	.770	6.83200E+04
.324	8.78750E+03	.467	3.86000E+04	.642	5.88050E+04	.787	6.92650E+04
.337	1.22750E+04	.477	4.00525E+04	.649	5.94050E+04	.792	6.95650E+04
.349	1.57625E+04	.486	4.14125E+04	.669	6.11150E+04	.797	6.98650E+04
.362	1.89125E+04	.495	4.26500E+04	.682	6.21350E+04	.804	7.02550E+04
.373	2.15000E+04	.521	4.59050E+04	.694	6.31550E+04		
.385	2.38625E+04	.538	4.80050E+04	.707	6.40850E+04		
.396	2.61125E+04	.554	4.99850E+04	.713	6.44750E+04		
.419	3.02750E+04	.569	5.16950E+04	.731	6.57550E+04		
.428	3.21875E+04	.577	5.25050E+04	.742	6.65350E+04		
.438	3.39875E+04	.600	5.48450E+04	.754	6.72850E+04		
.448	3.56750E+04	.614	5.62550E+04	.765	6.90050E+04		

Table 2 (continued)

SPECIMEN TI 5 ENVIRON. ARGON WIDTH = 3.000 IN. THICK. = .243 IN. TEMP. = 49.00 C
MAXIMUM LOAD =10.00 KIPS STRESS RATIO = .050 FREQUENCY = 5.0 HZ NO. OF POINTS = 40

CRACK LENGTH	NO. OF CYCLES	CRACK LENGTH	NO. OF CYCLES	CRACK LENGTH	NO. OF CYCLES	CRACK LENGTH	NO. OF CYCLES
.305	0.	.421	3.12325E+04	.604	5.75925E+04	.749	6.97475E+04
.312	2.25000E+03	.441	3.49325E+04	.618	5.90175E+04	.764	7.09375E+04
.323	5.62500E+03	.451	3.64075E+04	.625	5.97675E+04	.775	7.14775E+04
.332	8.25000E+03	.460	3.81325E+04	.645	6.17175E+04	.785	7.21175E+04
.340	1.11000E+04	.469	3.96325E+04	.658	6.29075E+04		
.344	1.22250E+04	.496	4.40175E+04	.671	6.39875E+04		
.356	1.56075E+04	.513	4.63050E+04	.683	6.50175E+04		
.364	1.75200E+04	.529	4.85925E+04	.690	6.54675E+04		
.375	2.05575E+04	.545	5.06550E+04	.708	6.69175E+04		
.383	2.24325E+04	.553	5.16675E+04	.713	6.77775E+04		
.401	2.67325E+04	.576	5.43675E+04	.731	6.96075E+04		
.411	2.89875E+04	.590	5.60175E+04	.742	6.93975E+04		

SPECIMEN TI 4 ENVIRON. ARGON WIDTH = 3.000 IN. THICK. = .245 IN. TEMP. = 49.00 C
MAXIMUM LOAD = 5.60 KIPS STRESS RATIO = .050 FREQUENCY =10.0 HZ NO. OF POINTS = 46

CRACK LENGTH	NO. OF CYCLES	CRACK LENGTH	NO. OF CYCLES	CRACK LENGTH	NO. OF CYCLES	CRACK LENGTH	NO. OF CYCLES
.380	0.	.469	2.67300E+05	.545	4.14100E+05	.701	4.93600E+05
.400	9.60000E+03	.478	2.99900E+05	.551	4.17700E+05	.712	4.87200E+05
.404	2.04000E+04	.484	3.20900E+05	.566	4.27650E+05	.724	4.90350E+05
.411	4.02000E+04	.490	3.35900E+05	.581	4.36050E+05	.736	4.93650E+05
.418	6.30000E+04	.496	3.51500E+05	.595	4.43400E+05	.741	4.95225E+05
.425	8.76000E+04	.499	3.58400E+05	.610	4.50300E+05	.758	4.99650E+05
.434	1.47000E+05	.507	3.74600E+05	.617	4.53450E+05	.769	5.02275E+05
.441	1.62000E+05	.513	3.82400E+05	.637	4.62000E+05	.779	5.04600E+05
.444	1.77000E+05	.518	3.89450E+05	.650	4.66950E+05	.790	5.06925E+05
.447	1.89600E+05	.524	3.95300E+05	.663	4.71600E+05	.800	5.09100E+05
.454	2.10900E+05	.535	4.05850E+05	.676	4.75875E+05		
.460	2.34000E+05	.540	4.10275E+05	.682	4.77825E+05		

Table 2 (continued)

SPECIMEN TI 3 ENVIRON. ARGON WIDTH = 3.000 IN. THICK. = .244 IN. TEMP. = 84.00 C
MAXIMUM LOAD = 8.00 KIPS STRESS RATIO = .050 FREQUENCY = 5.0 HZ NO. OF POINTS = 23

CRACK LENGTH	NO. OF CYCLES	CRACK LENGTH	NO. OF CYCLES	CRACK LENGTH	NO. OF CYCLES	CRACK LENGTH	NO. OF CYCLES
.445	0.	.601	4.80375E+04				
.454	4.20000E+03	.615	5.09625E+04				
.463	8.10000E+03	.628	5.35875E+04				
.472	1.15500E+04	.642	5.61375E+04				
.481	1.48500E+04	.662	5.96625E+04				
.490	1.80000E+04	.681	6.27375E+04				
.507	2.41500E+04	.699	6.55125E+04				
.524	2.91000E+04	.717	6.82125E+04				
.540	3.36000E+04	.734	7.04625E+04				
.556	3.76500E+04	.751	7.25625E+04				
.571	4.15500E+04	.776	7.54875E+04				
.586	4.50375E+04						

SPECIMEN TI 2 ENVIRON. ARGON WIDTH = 3.000 IN. THICK. = .239 IN. TEMP. = 91.20 C
MAXIMUM LOAD =14.00 KIPS STRESS RATIO = .050 FREQUENCY = 5.0 HZ NO. OF POINTS = 37

CRACK LENGTH	NO. OF CYCLES	CRACK LENGTH	NO. OF CYCLES	CRACK LENGTH	NO. OF CYCLES	CRACK LENGTH	NO. OF CYCLES
.286	0.	.452	1.55250E+04	.641	2.66700E+04	.735	3.05000E+04
.295	1.12500E+03	.471	1.68000E+04	.654	2.70300E+04		
.310	2.85000E+03	.490	1.80000E+04	.668	2.75100E+04		
.324	4.42500E+03	.509	1.93000E+04	.684	2.78900E+04		
.338	5.85000E+03	.526	2.02700E+04	.693	2.82300E+04		
.351	7.27500E+03	.543	2.11500E+04	.705	2.85700E+04		
.363	8.47500E+03	.553	2.34000E+04	.717	2.88900E+04		
.375	9.60000E+03	.569	2.40700E+04	.729	2.91800E+04		
.387	1.05750E+04	.584	2.46500E+04	.741	2.94700E+04		
.398	1.15500E+04	.599	2.51900E+04	.752	2.97800E+04		
.410	1.24500E+04	.613	2.57300E+04	.763	3.00400E+04		
.431	1.41000E+04	.627	2.62000E+04	.774	3.02800E+04		

Table 2 (continued)

SPECIMEN TI 30 ENVIRON. ARGON WIDTH = 3.000 IN. THICK. = .241 IN. TEMP. =100.40 C
MAXIMUM LOAD = 8.00 KIPS STRESS RATIO = .050 FREQUENCY = 5.0 HZ NO. OF POINTS = 19

CRACK LENGTH	NO. OF CYCLES	CRACK LENGTH	NO. OF CYCLES	CRACK LENGTH	NO. OF CYCLES	CRACK LENGTH	NO. OF CYCLES
.409	4.87000E+03	.480	3.65975E+04				
.416	8.62000E+03	.489	3.99625E+04				
.419	1.04950E+04	.495	4.18750E+04				
.426	1.26625E+04	.500	4.38625E+04				
.433	1.69000E+04	.506	4.56250E+04				
.439	1.99750E+04	.509	4.64375E+04				
.446	2.28625E+04	.517	4.91500E+04				
.449	2.41375E+04						
.458	2.82625E+04						
.465	3.07375E+04						
.471	3.31250E+04						
.477	3.55000E+04						

SPECIMEN TI 30 ENVIRON. ARGON WIDTH = 3.000 IN. THICK. = .241 IN. TEMP. = 95.00 C
MAXIMUM LOAD = 5.00 KIPS STRESS RATIO = .050 FREQUENCY = 5.0 HZ NO. OF POINTS = 11

CRACK LENGTH	NO. OF CYCLES	CRACK LENGTH	NO. OF CYCLES	CRACK LENGTH	NO. OF CYCLES	CRACK LENGTH	NO. OF CYCLES
.543	3.45000E+04						
.552	6.30000E+04						
.557	1.05000E+05						
.560	1.20000E+05						
.570	1.44000E+05						
.573	1.58400E+05						
.575	1.70400E+05						
.578	1.83600E+05						
.580	1.97100E+05						
.583	2.11800E+05						
.585	2.23500E+05						

Table 2 (continued)

SPECIMEN TI 30 ENVIRON. ARGON WIDTH = 3.000 IN. THICK. = .241 IN. TEMP. = 92.00 C
MAXIMUM LOAD = 5.80 KIPS STRESS RATIO = .050 FREQUENCY = 5.0 HZ NO. OF POINTS = 28

CRACK LENGTH	NO. OF CYCLES	CRACK LENGTH	NO. OF CYCLES	CRACK LENGTH	NO. OF CYCLES	CRACK LENGTH	NO. OF CYCLES
.592	2.50000E+02	.641	5.29000E+04	.749	1.15825E+05		
.595	2.95000E+03	.645	5.65000E+04	.760	1.21175E+05		
.597	5.65000E+03	.650	5.97250E+04	.770	1.25525E+05		
.602	1.19500E+04	.656	6.48625E+04	.780	1.29200E+05		
.604	1.52500E+04	.663	6.93625E+04				
.607	1.90000E+04	.669	7.36750E+04				
.609	2.27500E+04	.678	7.95250E+04				
.614	2.90500E+04	.690	8.65750E+04				
.618	3.44500E+04	.702	9.31750E+04				
.623	3.88000E+04	.714	9.94750E+04				
.628	4.30000E+04	.720	1.02475E+05				
.637	4.92250E+04	.737	1.11800E+05				

SPECIMEN TI 18 ENVIRON. ARGON WIDTH = 3.000 IN. THICK. = .241 IN. TEMP. =131.00 C
MAXIMUM LOAD =10.00 KIPS STRESS RATIO = .050 FREQUENCY = 5.0 HZ NO. OF POINTS = 30

CRACK LENGTH	NO. OF CYCLES	CRACK LENGTH	NO. OF CYCLES	CRACK LENGTH	NO. OF CYCLES	CRACK LENGTH	NO. OF CYCLES
.293	0.	.464	4.89750E+04	.674	7.56000E+04		
.299	2.70000E+03	.481	5.20500E+04	.691	7.71000E+04		
.312	7.50000E+03	.498	5.46750E+04	.708	7.84200E+04		
.324	1.20000E+04	.513	5.70750E+04	.724	7.96800E+04		
.336	1.65000E+04	.529	5.93250E+04	.740	8.08900E+04		
.346	2.02500E+04	.544	6.14250E+04	.761	8.23000E+04		
.359	2.34000E+04	.558	6.33750E+04				
.370	2.68500E+04	.579	6.59250E+04				
.390	3.29250E+04	.599	6.82500E+04				
.414	3.76500E+04	.619	7.04250E+04				
.429	4.19250E+04	.638	7.23000E+04				
.447	4.56000E+04	.656	7.40250E+04				

Table 2 (continued)

SPECIMEN TI 28 ENVIRON. ARGON WIDTH = 3.000 IN. THICK. = .243 IN. TEMP. =140.00 C
MAXIMUM LOAD = 9.00 KIPS STRESS RATIO = .050 FREQUENCY = 5.0 HZ NO. OF POINTS = 48

CRACK LENGTH	NO. OF CYCLES	CRACK LENGTH	NO. OF CYCLES	CRACK LENGTH	NO. OF CYCLES	CRACK LENGTH	NO. OF CYCLES
.328	4.50000E+03	.412	6.16125E+04	.522	9.67375E+04	.663	1.21187E+05
.333	1.00500E+04	.415	6.30000E+04	.530	9.84625E+04	.675	1.22752E+05
.337	1.53000E+04	.418	6.42750E+04	.552	1.03337E+05	.681	1.23550E+05
.340	1.98000E+04	.434	7.03500E+04	.559	1.04687E+05	.698	1.25725E+05
.352	3.03000E+04	.440	7.35000E+04	.571	1.06487E+05	.710	1.27075E+05
.367	3.97500E+04	.446	7.54500E+04	.578	1.07837E+05	.721	1.28275E+05
.371	4.18500E+04	.452	7.75125E+04	.585	1.09112E+05	.732	1.29512E+05
.374	4.41000E+04	.459	7.93125E+04	.599	1.11437E+05	.737	1.30112E+05
.381	4.79250E+04	.481	9.63125E+04	.612	1.13650E+05	.753	1.31752E+05
.388	5.15250E+04	.490	8.87125E+04	.619	1.14625E+05	.763	1.32732E+05
.395	5.47500E+04	.498	9.08125E+04	.638	1.17737E+05	.773	1.33712E+05
.402	5.76750E+04	.506	9.29125E+04	.650	1.19875E+05	.793	1.34622E+05
.412	6.16125E+04	.522	9.67375E+04	.663	1.21187E+05		

SPECIMEN TI 12 ENVIRON. ARGON WIDTH = 3.000 IN. THICK. = .224 IN. TEMP. =141.00 C
MAXIMUM LOAD =14.00 KIPS STRESS RATIO = .050 FREQUENCY = 5.0 HZ NO. OF POINTS = 22

CRACK LENGTH	NO. OF CYCLES	CRACK LENGTH	NO. OF CYCLES	CRACK LENGTH	NO. OF CYCLES	CRACK LENGTH	NO. OF CYCLES
.452	1.00000E+02	.545	4.80000E+03				
.460	5.60000E+02	.552	5.10000E+03				
.468	1.03000E+03	.565	5.74000E+03				
.476	1.46000E+03	.573	6.28000E+03				
.485	1.93000E+03	.592	6.77000E+03				
.492	2.35000E+03	.605	7.25000E+03				
.500	2.75000E+03	.617	7.71000E+03				
.508	3.12000E+03	.630	8.19000E+03				
.515	3.49000E+03	.642	8.59000E+03				
.523	3.83000E+03	.654	9.01000E+03				
.530	4.16000E+03						
.537	4.49000E+03						

Table 2 (continued)

SPECIMEN TI 1 ENVIRON. ARGON WIDTH = 3.000 IN. THICK. = .233 IN. TEMP. =140.00 C
MAXIMUM LOAD = 6.60 KIPS STRESS RATIO = .050 FREQUENCY =10.0 HZ NO. OF POINTS = 47

CRACK LENGTH	NO. OF CYCLES	CRACK LENGTH	NO. OF CYCLES	CRACK LENGTH	NO. OF CYCLES	CRACK LENGTH	NO. OF CYCLES
.315	0.	.389	3.40800E+05	.474	4.70550E+05	.613	5.45400E+05
.320	7.29000E+04	.396	3.59100E+05	.480	4.75325E+05	.633	5.52375E+05
.326	1.00800E+05	.403	3.73200E+05	.485	4.79375E+05	.652	5.58600E+05
.332	1.27200E+05	.409	3.86700E+05	.491	4.83500E+05	.664	5.62350E+05
.343	1.73400E+05	.416	3.99600E+05	.497	4.87325E+05	.676	5.66025E+05
.347	1.86300E+05	.419	4.05600E+05	.510	4.96125E+05	.688	5.69325E+05
.356	2.23200E+05	.432	4.17300E+05	.518	5.01525E+05	.694	5.70825E+05
.364	2.58300E+05	.438	4.26750E+05	.534	5.10225E+05	.711	5.75250E+05
.371	2.85600E+05	.448	4.34250E+05	.549	5.18025E+05	.722	5.77950E+05
.375	2.98500E+05	.457	4.44900E+05	.564	5.25075E+05	.733	5.80500E+05
.378	3.09900E+05	.463	4.55700E+05	.586	5.34675E+05	.739	5.81775E+05
.382	3.21300E+05	.468	4.61100E+05	.599	5.40300E+05		

SPECIMEN TI 21 ENVIRON. ARGON WIDTH = 3.000 IN. THICK. = .237 IN. TEMP. =204.20 C
MAXIMUM LOAD =10.00 KIPS STRESS RATIO = .050 FREQUENCY = 5.0 HZ NO. OF POINTS = 36

CRACK LENGTH	NO. OF CYCLES	CRACK LENGTH	NO. OF CYCLES	CRACK LENGTH	NO. OF CYCLES	CRACK LENGTH	NO. OF CYCLES
.292	0.	.444	5.23500E+04	.630	8.03000E+04		
.343	2.59750E+04	.470	5.75375E+04	.642	8.16500E+04		
.347	2.71750E+04	.487	6.06875E+04	.654	8.28500E+04		
.350	2.84125E+04	.503	6.33875E+04	.661	8.33375E+04		
.354	2.95750E+04	.518	6.59000E+04	.678	8.50575E+04		
.358	3.06250E+04	.526	6.69500E+04	.690	8.61175E+04		
.376	3.60750E+04	.549	7.02500E+04	.701	8.70975E+04		
.396	4.17000E+04	.563	7.22000E+04	.712	8.80175E+04		
.406	4.43250E+04	.577	7.41500E+04	.718	8.84675E+04		
.416	4.64250E+04	.591	7.58375E+04	.734	8.97775E+04		
.425	4.84500E+04	.597	7.66250E+04	.739	9.01875E+04		
.435	5.03250E+04	.617	7.89125E+04	.744	9.06075E+04		

Table 2 (continued)

SPECIMEN TI 11 ENVIRON. ARGON WIDTH = 3.004 IN. THICK. = .227 IN. TEMP. =210.00 C
MAXIMUM LOAD = 6.00 KIPS STRESS RATIO = .050 FREQUENCY =10.0 HZ NO. OF POINTS = 38

CRACK LENGTH	NO. OF CYCLES	CRACK LENGTH	NO. OF CYCLES	CRACK LENGTH	NO. OF CYCLES	CRACK LENGTH	NO. OF CYCLES
.288	0.	.425	5.08500E+05	.609	7.96750E+05	.756	8.49275E+05
.313	3.90000E+04	.435	5.33700E+05	.621	7.94100E+05	.760	8.50625E+05
.319	6.79000E+04	.452	5.76900E+05	.627	7.97850E+05		
.325	9.42000E+04	.469	6.21900E+05	.646	8.07050E+05		
.331	1.20600E+05	.486	6.50100E+05	.658	8.12675E+05		
.337	1.47000E+05	.510	6.88700E+05	.669	8.18075E+05		
.348	2.25000E+05	.525	7.10900E+05	.681	8.23175E+05		
.359	2.71800E+05	.540	7.29800E+05	.687	8.25275E+05		
.370	3.15000E+05	.554	7.46300E+05	.703	8.31800E+05		
.380	3.57000E+05	.561	7.52300E+05	.714	8.35775E+05		
.400	4.24200E+05	.582	7.68150E+05	.730	8.41100E+05		
.410	4.61400E+05	.595	7.78350E+05	.741	8.44550E+05		

SPECIMEN TI 9 ENVIRON. ARGON WIDTH = 3.005 IN. THICK. = .240 IN. TEMP. =291.40 C
MAXIMUM LOAD =10.00 KIPS STRESS RATIO = .050 FREQUENCY = 5.0 HZ NO. OF POINTS = 38

CRACK LENGTH	NO. OF CYCLES	CRACK LENGTH	NO. OF CYCLES	CRACK LENGTH	NO. OF CYCLES	CRACK LENGTH	NO. OF CYCLES
.321	0.	.469	3.54600E+04	.662	5.85250E+04	.802	6.93275E+04
.340	8.55000E+03	.496	3.91750E+04	.675	5.97625E+04	.807	6.95475E+04
.353	1.18500E+04	.514	4.17625E+04	.688	6.09500E+04		
.365	1.48500E+04	.531	4.40125E+04	.694	6.13375E+04		
.377	1.75500E+04	.547	4.61125E+04	.712	6.28375E+04		
.399	2.27850E+04	.555	4.70875E+04	.724	6.38175E+04		
.410	2.49600E+04	.578	4.98250E+04	.736	6.47175E+04		
.420	2.69100E+04	.593	5.15125E+04	.748	6.55775E+04		
.430	2.90850E+04	.607	5.30875E+04	.753	6.60175E+04		
.440	3.05600E+04	.622	5.45500E+04	.770	6.71875E+04		
.450	3.23100E+04	.629	5.53000E+04	.781	6.79475E+04		
.460	3.38950E+04	.649	5.73625E+04	.791	6.86575E+04		

Table 2 (continued)

SPECIMEN TI 22 ENVIRON. ARGON WIDTH = 3.000 IN. THICK. = .235 IN. TEMP. =296.50 C
MAXIMUM LOAD = 6.60 KIPS STRESS RATIO = .050 FREQUENCY =10.0 HZ NO. OF POINTS = 43

CRACK LENGTH	NO. OF CYCLES	CRACK LENGTH	NO. OF CYCLES	CRACK LENGTH	NO. OF CYCLES	CRACK LENGTH	NO. OF CYCLES
.321	0.	.421	2.62200E+05	.595	4.71000E+05	.733	5.21875E+05
.328	8.40000E+03	.436	2.97600E+05	.608	4.77150E+05	.743	5.24200E+05
.334	3.00000E+04	.453	3.25200E+05	.620	4.82250E+05	.748	5.25400E+05
.339	4.80000E+04	.470	3.57600E+05	.633	4.87350E+05	.762	5.29000E+05
.345	6.60000E+04	.478	3.69600E+05	.633	4.89900E+05	.772	5.31250E+05
.351	8.22000E+04	.491	3.84600E+05	.655	4.95750E+05	.782	5.33425E+05
.356	9.84000E+04	.507	4.01400E+05	.668	5.01250E+05	.791	5.35525E+05
.373	1.46400E+05	.527	4.21200E+05	.679	5.05375E+05		
.383	1.72800E+05	.541	4.34100E+05	.690	5.09275E+05		
.393	1.98000E+05	.555	4.45200E+05	.695	5.11000E+05		
.403	2.20200E+05	.569	4.56300E+05	.712	5.15800E+05		
.412	2.42400E+05	.576	4.60500E+05	.722	5.18800E+05		

Table 3: Fatigue-Crack Growth in Distilled Water at Two Test Temperatures

SPECIMEN TI 23 ENVIRON. WATER WIDTH = 3.000 IN. THICK. = .234 IN. TEMP. = 24.90 C
MAXIMUM LOAD =12.00 KIPS STRESS RATIO = .050 FREQUENCY = 5.0 HZ NO. OF POINTS = 17

CRACK LENGTH	NO. OF CYCLES	CRACK LENGTH	NO. OF CYCLES	CRACK LENGTH	NO. OF CYCLES	CRACK LENGTH	NO. OF CYCLES
.427	0.	.639	1.07000E+04				
.462	6.02500E+02	.658	1.14400E+04				
.471	1.31500E+03	.677	1.21200E+04				
.480	1.99000E+03	.695	1.27200E+04				
.488	2.66500E+03	.703	1.30200E+04				
.497	3.19000E+03						
.503	3.79000E+03						
.522	4.85000E+03						
.553	6.63000E+03						
.576	7.62000E+03						
.598	8.92000E+03						
.618	9.64000E+03						

SPECIMEN TI 6 ENVIRON. WATER WIDTH = 3.005 IN. THICK. = .240 IN. TEMP. = 25.50 C
MAXIMUM LOAD =10.00 KIPS STRESS RATIO = .050 FREQUENCY = 5.0 HZ NO. OF POINTS = 31

CRACK LENGTH	NO. OF CYCLES	CRACK LENGTH	NO. OF CYCLES	CRACK LENGTH	NO. OF CYCLES	CRACK LENGTH	NO. OF CYCLES
.324	0.	.557	2.94000E+04	.722	3.96675E+04		
.326	3.75000E+02	.571	3.05250E+04	.733	4.01775E+04		
.349	5.17500E+03	.585	3.15375E+04	.744	4.06275E+04		
.372	9.00000E+03	.599	3.25575E+04	.755	4.10575E+04		
.393	1.17000E+04	.613	3.34775E+04	.760	4.13575E+04		
.413	1.57500E+04	.626	3.43275E+04	.775	4.18975E+04		
.451	1.91250E+04	.645	3.55075E+04	.786	4.23075E+04		
.469	2.13000E+04	.664	3.66475E+04				
.486	2.32125E+04	.676	3.73275E+04				
.503	2.48625E+04	.688	3.79475E+04				
.532	2.70750E+04	.699	3.85675E+04				
.542	2.82000E+04	.705	3.88375E+04				

Table 3 (continued)

SPECIMEN TI 10 ENVIROM. WATER WIDTH = 3.010 IN. THICK. = .229 IN. TEMP. = 83.00 C
MAXIMUM LOAD =10.00 KIPS STRESS RATIO = .050 FREQUENCY = 5.0 HZ NO. OF POINTS = 19

CRACK LENGTH	NO. OF CYCLES	CRACK LENGTH	NO. OF CYCLES	CRACK LENGTH	NO. OF CYCLES	CRACK LENGTH	NO. OF CYCLES
.306	0.	.476	2.71875E+04				
.312	3.37500E+03	.484	2.84625E+04				
.325	5.77500E+03	.509	3.04875E+04				
.337	8.02500E+03	.524	3.18750E+04				
.348	9.90000E+03	.540	3.31500E+04				
.360	1.18500E+04	.555	3.44625E+04				
.371	1.35000E+04	.562	3.48750E+04				
.381	1.51500E+04						
.392	1.67250E+04						
.422	2.10000E+04						
.440	2.33625E+04						
.458	2.53375E+04						

SPECIMEN TI 10 ENVIRON. WATER WIDTH = 3.010 IN. THICK. = .229 IN. TEMP. = 83.00 C
MAXIMUM LOAD =12.00 KIPS STRESS RATIO = .050 FREQUENCY = 5.0 HZ NO. OF POINTS = 20

CRACK LENGTH	NO. OF CYCLES	CRACK LENGTH	NO. OF CYCLES	CRACK LENGTH	NO. OF CYCLES	CRACK LENGTH	NO. OF CYCLES
.583	6.70000E+02	.730	6.32500E+03				
.597	1.32000E+03	.741	6.65000E+03				
.610	1.92000E+03	.746	6.81500E+03				
.624	2.47000E+03	.762	7.27500E+03				
.630	2.76000E+03	.772	7.56000E+03				
.649	3.51000E+03	.782	7.83500E+03				
.661	3.99000E+03	.792	8.09000E+03				
.673	4.43000E+03	.797	8.21500E+03				
.685	4.86000E+03						
.691	5.06000E+03						
.708	5.62500E+03						
.719	5.98500E+03						

Table 4: Fatigue-Crack Growth in Dehumidified Oxygen at Two Test Temperatures

SPECIMEN TI 33 ENVIRON. OXYGEN WIDTH = 3.003 IN. THICK. = .234 IN. TEMP. = 25.00 C
MAXIMUM LOAD =10.00 KIPS STRESS RATIO = .050 FREQUENCY = 5.0 HZ NO. OF POINTS = 36

CRACK LENGTH	NO. OF CYCLES	CRACK LENGTH	NO. OF CYCLES	CRACK LENGTH	NO. OF CYCLES	CRACK LENGTH	NO. OF CYCLES
.323	2.61000E+03	.471	3.45375E+04	.658	5.60375E+04		
.336	5.98500E+03	.497	3.86000E+04	.671	5.70875E+04		
.348	9.21000E+03	.514	4.08500E+04	.683	5.81000E+04		
.360	1.25625E+04	.530	4.28750E+04	.690	5.85125E+04		
.367	1.45125E+04	.546	4.47500E+04	.707	5.90825E+04		
.375	5.13750E+03	.554	4.56875E+04	.719	5.99325E+04		
.382	6.97500E+03	.576	4.81250E+04	.730	6.07025E+04		
.389	1.98375E+04	.591	4.96625E+04	.742	6.14525E+04		
.404	2.32875E+04	.605	5.10875E+04	.747	6.17825E+04		
.424	2.74125E+04	.619	5.24750E+04	.764	6.27725E+04		
.443	3.08625E+04	.626	5.31500E+04	.774	6.34025E+04		
.462	3.37875E+04	.646	5.49125E+04	.779	6.36925E+04		

SPECIMEN TI 32 ENVIRON. OXYGEN WIDTH = .300 IN. THICK. = .244 IN. TEMP. =130.00 C
MAXIMUM LOAD =10.00 KIPS STRESS RATIO = .050 FREQUENCY = 5.0 HZ NO. OF POINTS = 36

CRACK LENGTH	NO. OF CYCLES	CRACK LENGTH	NO. OF CYCLES	CRACK LENGTH	NO. OF CYCLES	CRACK LENGTH	NO. OF CYCLES
.312	0.	.514	4.80000E+04	.682	6.69000E+04		
.325	4.80000E+03	.530	5.03250E+04	.688	6.74250E+04		
.338	9.15000E+03	.546	5.24250E+04	.706	6.88350E+04		
.350	1.29000E+04	.554	5.34000E+04	.718	6.97450E+04		
.361	1.65000E+04	.576	5.61750E+04	.729	7.06150E+04		
.373	1.96500E+04	.590	5.78250E+04	.740	7.14350E+04		
.394	2.52000E+04	.605	5.94375E+04	.746	7.18350E+04		
.415	3.03750E+04	.618	6.09000E+04	.762	7.29450E+04		
.435	3.42750E+04	.625	6.15750E+04	.772	7.36650E+04		
.454	3.78750E+04	.645	6.35250E+04	.783	7.43550E+04		
.472	4.12500E+04	.658	6.47250E+04	.793	7.50250E+04		
.498	4.54500E+04	.670	6.58125E+04	.798	7.53350E+04		

Table 5: Fatigue-Crack Growth in Dehumidified Hydrogen at Room Temperature

SPECIMEN TI 17 ENVIRON. HYDROGEN WIDTH = 3.000 IN. THICK. = .236 IN. TEMP. = 22.50 C
MAXIMUM LOAD =14.00 KIPS STRESS RATIO = .050 FREQUENCY = 5.0 HZ NO. OF POINTS = 21

CRACK LENGTH	NO. OF CYCLES	CRACK LENGTH	NO. OF CYCLES	CRACK LENGTH	NO. OF CYCLES	CRACK LENGTH	NO. OF CYCLES
.474	3.00000E+02	.644	8.48000E+03				
.493	1.08000E+03	.657	8.92000E+03				
.502	1.62000E+03	.670	9.33000E+03				
.510	2.15000E+03	.695	1.00950E+04				
.519	2.65000E+03	.707	1.04300E+04				
.527	3.13000E+03	.719	1.07800E+04				
.535	3.58000E+03	.731	1.10250E+04				
.559	4.84000E+03	.753	1.15750E+04				
.574	5.58000E+03	.760	1.17250E+04				
.589	6.23000E+03						
.603	6.88000E+03						
.631	7.98000E+03						

SPECIMEN TI 20 ENVIRON. HYDROGEN WIDTH = 3.005 IN. THICK. = .233 IN. TEMP. = 25.50 C
MAXIMUM LOAD =10.00 KIPS STRESS RATIO = .050 FREQUENCY = 5.0 HZ NO. OF POINTS = 38

CRACK LENGTH	NO. OF CYCLES	CRACK LENGTH	NO. OF CYCLES	CRACK LENGTH	NO. OF CYCLES	CRACK LENGTH	NO. OF CYCLES
.337	6.00000E+02	.497	2.99500E+04	.661	4.45300E+04	.804	5.29600E+04
.368	7.67500E+03	.506	3.10375E+04	.680	4.58400E+04	.814	5.34500E+04
.379	1.02250E+04	.514	3.20500E+04	.693	4.66400E+04		
.390	1.24000E+04	.539	3.47875E+04	.705	4.73900E+04		
.401	1.47250E+04	.555	3.63250E+04	.717	4.81300E+04		
.412	1.68250E+04	.570	3.76375E+04	.723	4.84600E+04		
.422	1.86250E+04	.585	3.88000E+04	.740	4.95200E+04		
.452	2.35375E+04	.593	3.94000E+04	.751	5.01600E+04		
.461	2.50000E+04	.614	4.10700E+04	.762	5.07800E+04		
.470	2.62750E+04	.628	4.21100E+04	.773	5.13300E+04		
.480	2.76250E+04	.641	4.31300E+04	.778	5.16200E+04		
.488	2.88250E+04	.655	4.40800E+04	.794	5.24400E+04		

Table 6: Fatigue-Crack Growth in Vacuum and in Distilled Water (NASA Langley Research Center Data)

SPECIMEN TI 25 ENVIRON. VACCUM WIDTH = 2.990 IN. THICK. = .238 IN. TEMP. = 25.00 C
MAXIMUM LOAD =18.29 KIPS STRESS RATIO = .050 FREQUENCY =16.7 HZ NO. OF POINTS = 18

CRACK LENGTH	NO. OF CYCLES	CRACK LENGTH	NO. OF CYCLES	CRACK LENGTH	NO. OF CYCLES	CRACK LENGTH	NO. OF CYCLES
.365	2.24000E+04	.550	4.64000E+04	.850	5.98000E+04	.950	1.59300E+05
.400	2.90000E+04	.600	5.01000E+04	.900	6.05000E+04	1.000	1.61200E+05
.425	3.28000E+04	.650	5.29000E+04	.950	6.11000E+04	1.050	1.62500E+05
.450	3.64000E+04	.700	5.53300E+04	1.000	6.14000E+04	1.100	1.63500E+05
.475	3.96000E+04	.750	5.74000E+04	1.050	6.16000E+04	1.170	1.64400E+05
.500	4.20000E+04	.800	5.88000E+04	1.100	6.17000E+04		

SPECIMEN TI 13 ENVIRON. VACCUM WIDTH = 2.990 IN. THICK. = .238 IN. TEMP. = 25.00 C
MAXIMUM LOAD =14.05 KIPS STRESS RATIO = .050 FREQUENCY =10.0 HZ NO. OF POINTS = 23

CRACK LENGTH	NO. OF CYCLES	CRACK LENGTH	NO. OF CYCLES	CRACK LENGTH	NO. OF CYCLES	CRACK LENGTH	NO. OF CYCLES
.330	2.00000E+03	.475	7.90000E+04	.650	1.28500E+05	.950	1.59300E+05
.350	1.40000E+04	.500	8.90000E+04	.700	1.36700E+05	1.000	1.61200E+05
.380	3.20000E+04	.525	9.75000E+04	.750	1.43600E+05	1.050	1.62500E+05
.400	4.35000E+04	.550	1.05500E+05	.800	1.49200E+05	1.100	1.63500E+05
.430	5.90000E+04	.575	1.13000E+05	.850	1.53500E+05	1.170	1.64400E+05
.450	6.85000E+04	.600	1.19000E+05	.900	1.56700E+05		

Table 6 (continued)

SPECIMEN TI 26 ENVIRON. VACCUM WIDTH = 2.990 IN. THICK. = .244 IN. TEMP. =-61.00 C
MAXIMUM LOAD =18.62 KIPS STRESS RATIO = .050 FREQUENCY =15.0 HZ NO. OF POINTS = 18

CRACK LENGTH	NO. OF CYCLES	CRACK LENGTH	NO. OF CYCLES	CRACK LENGTH	NO. OF CYCLES	CRACK LENGTH	NO. OF CYCLES
.350	1.40000E+04	.500	3.60000E+04	.800	5.19000E+04	.950	1.59300E+05
.375	1.85000E+04	.550	4.06000E+04	.850	5.27000E+04	1.000	1.61200E+05
.400	2.28000E+04	.600	4.42000E+04	.900	5.33000E+04	1.050	1.62500E+05
.425	2.65000E+04	.650	4.70000E+04	.950	5.36000E+04	1.100	1.63500E+05
.450	3.02000E+04	.700	4.82000E+04	1.000	5.38000E+04	1.170	1.64400E+05
.475	3.33000E+04	.750	5.08000E+04	1.100	5.40000E+04		

SPECIMEN TI 31 ENVIRON. WATER WIDTH = 3.000 IN. THICK. = .239 IN. TEMP. = 25.00 C
MAXIMUM LOAD =14.05 KIPS STRESS RATIO = .050 FREQUENCY = 5.0 HZ NO. OF POINTS = 17

CRACK LENGTH	NO. OF CYCLES	CRACK LENGTH	NO. OF CYCLES	CRACK LENGTH	NO. OF CYCLES	CRACK LENGTH	NO. OF CYCLES
.320	4.00000E+03	.620	4.22000E+04	.920	5.59500E+04	.950	1.59300E+05
.370	1.40000E+04	.670	4.65000E+04	.970	5.71000E+04	1.000	1.61200E+05
.420	2.18000E+04	.720	4.83000E+04	1.020	5.80000E+04	1.050	1.62500E+05
.470	2.82000E+04	.770	5.07000E+04	1.070	5.88000E+04	1.100	1.63500E+05
.520	3.37000E+04	.820	5.27000E+04	1.110	5.92000E+04	1.170	1.64400E+05
.570	3.84000E+04	.870	5.44500E+04	1.100	6.17000E+04		

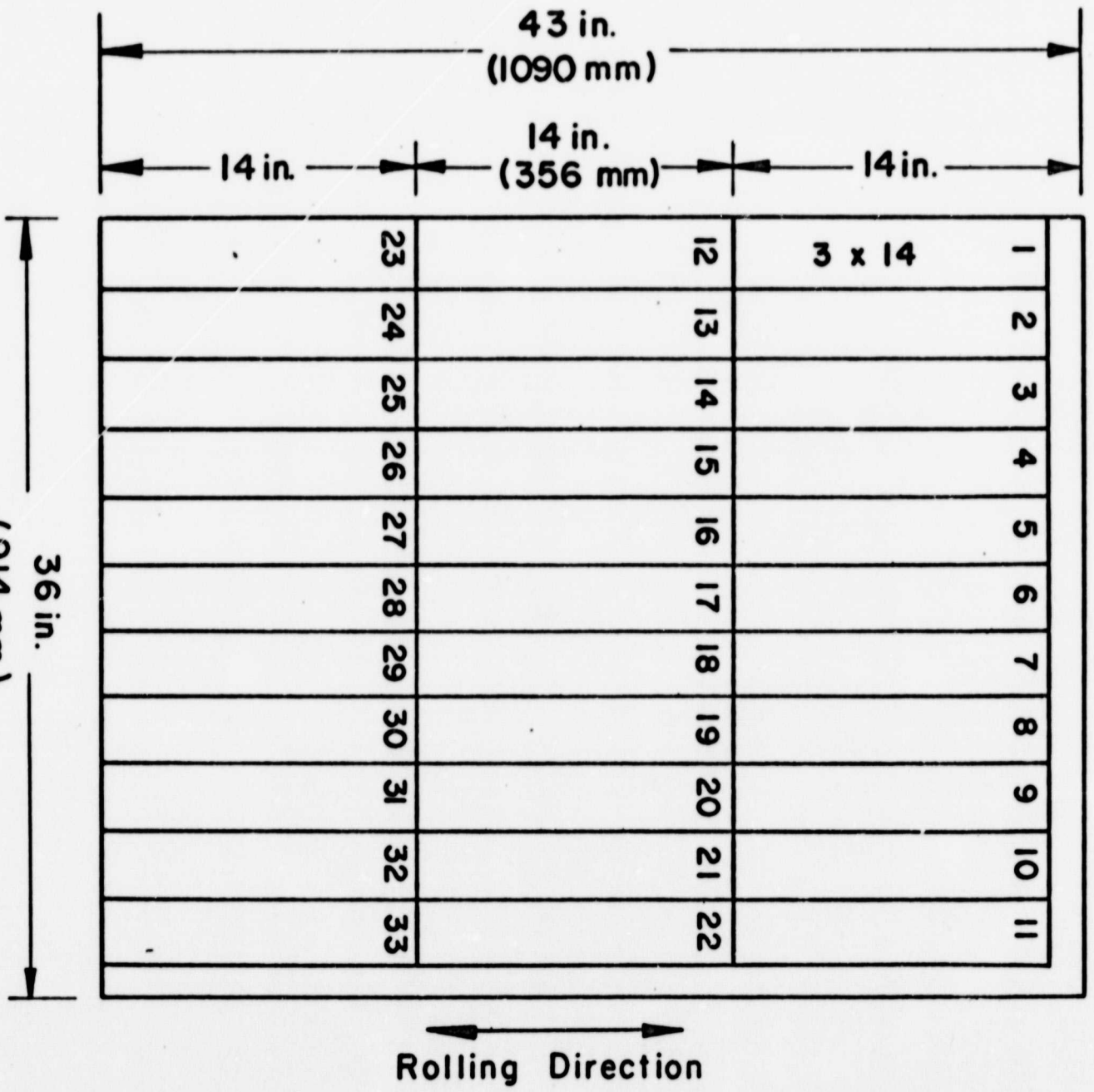

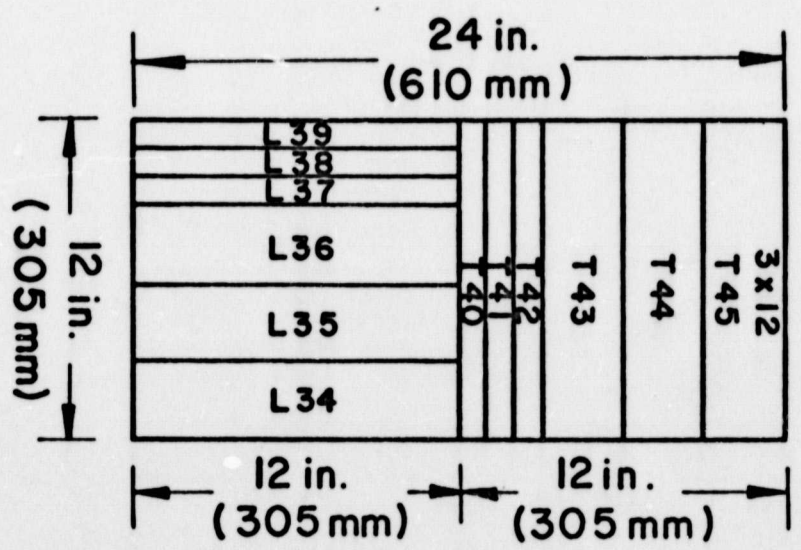

Figure 1: Specimen layout

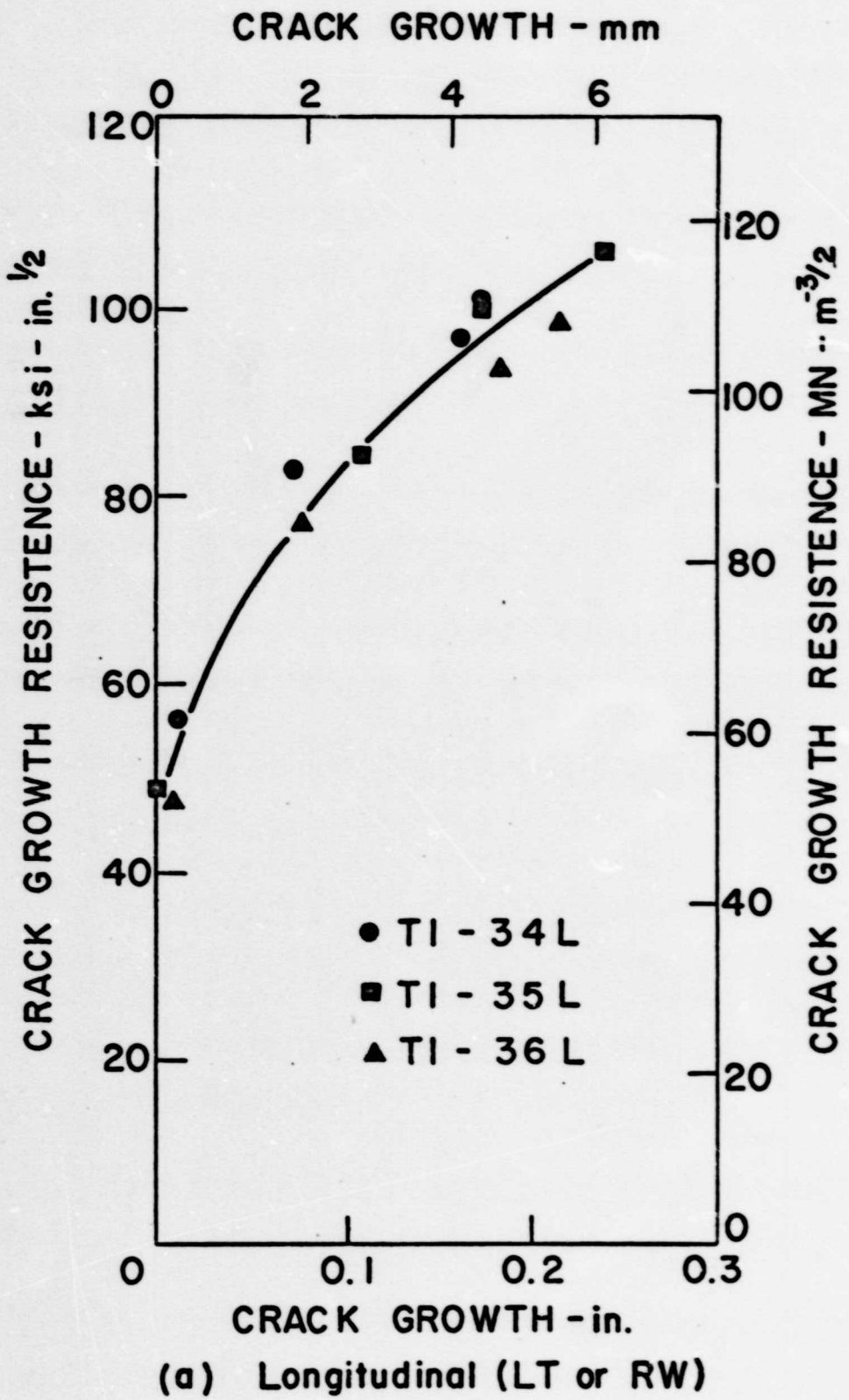

(a) Longitudinal (LT or RW)

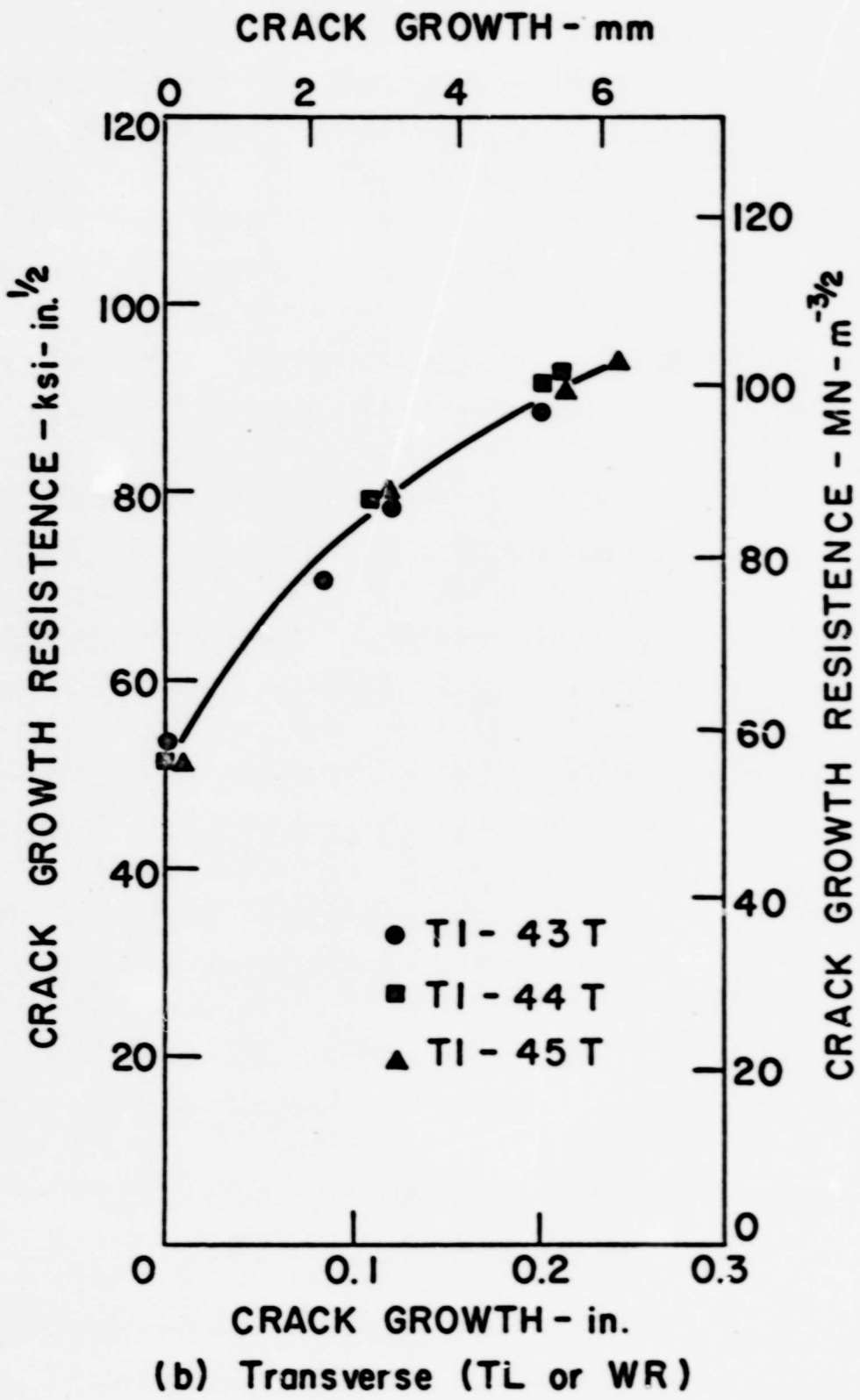

(b) Transverse (TL or WR)

Figure 8. Crack growth resistance curves for

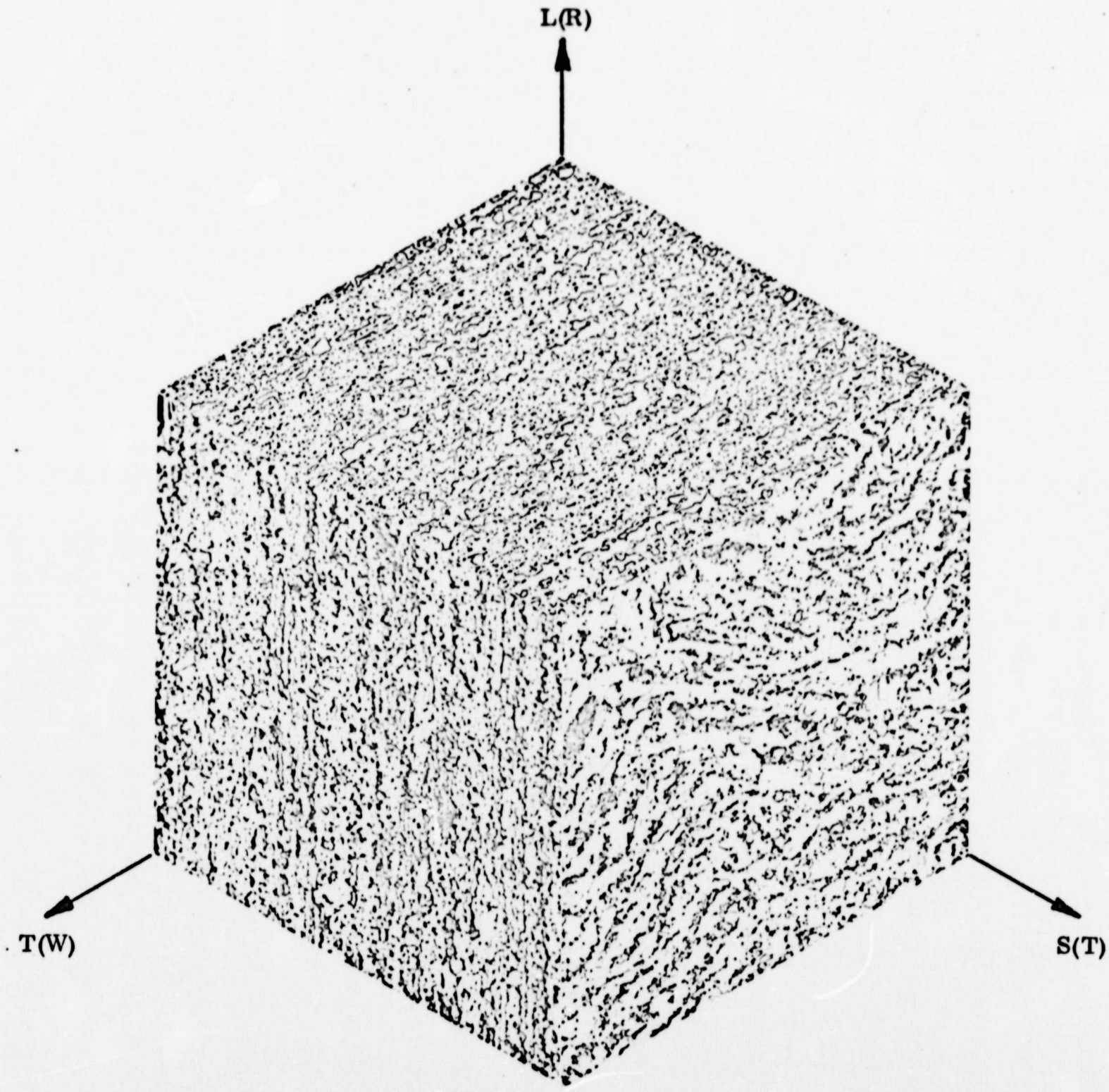

Figure 3: Representative microstructure of alloy investigated (200X)

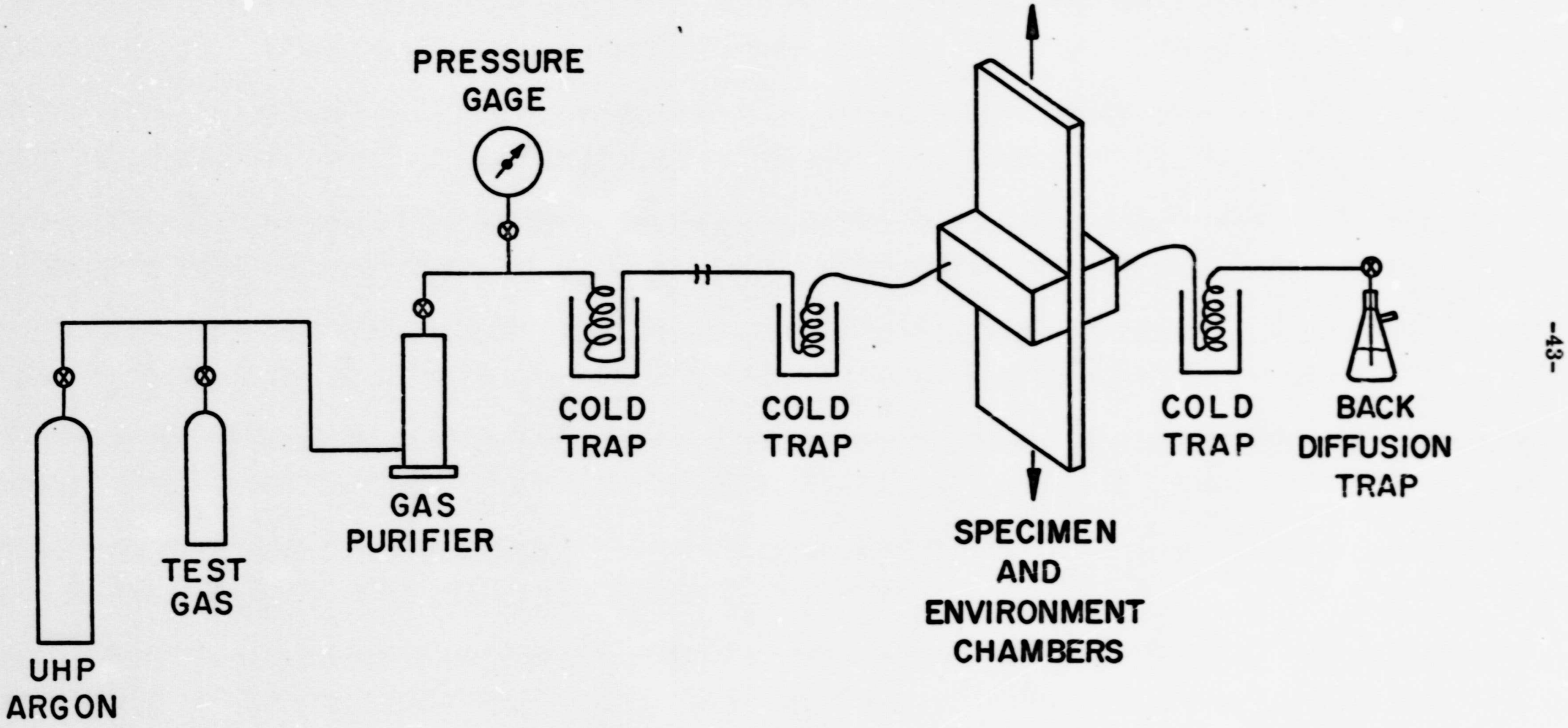

Figure 4: Schematic diagram of environmental control system

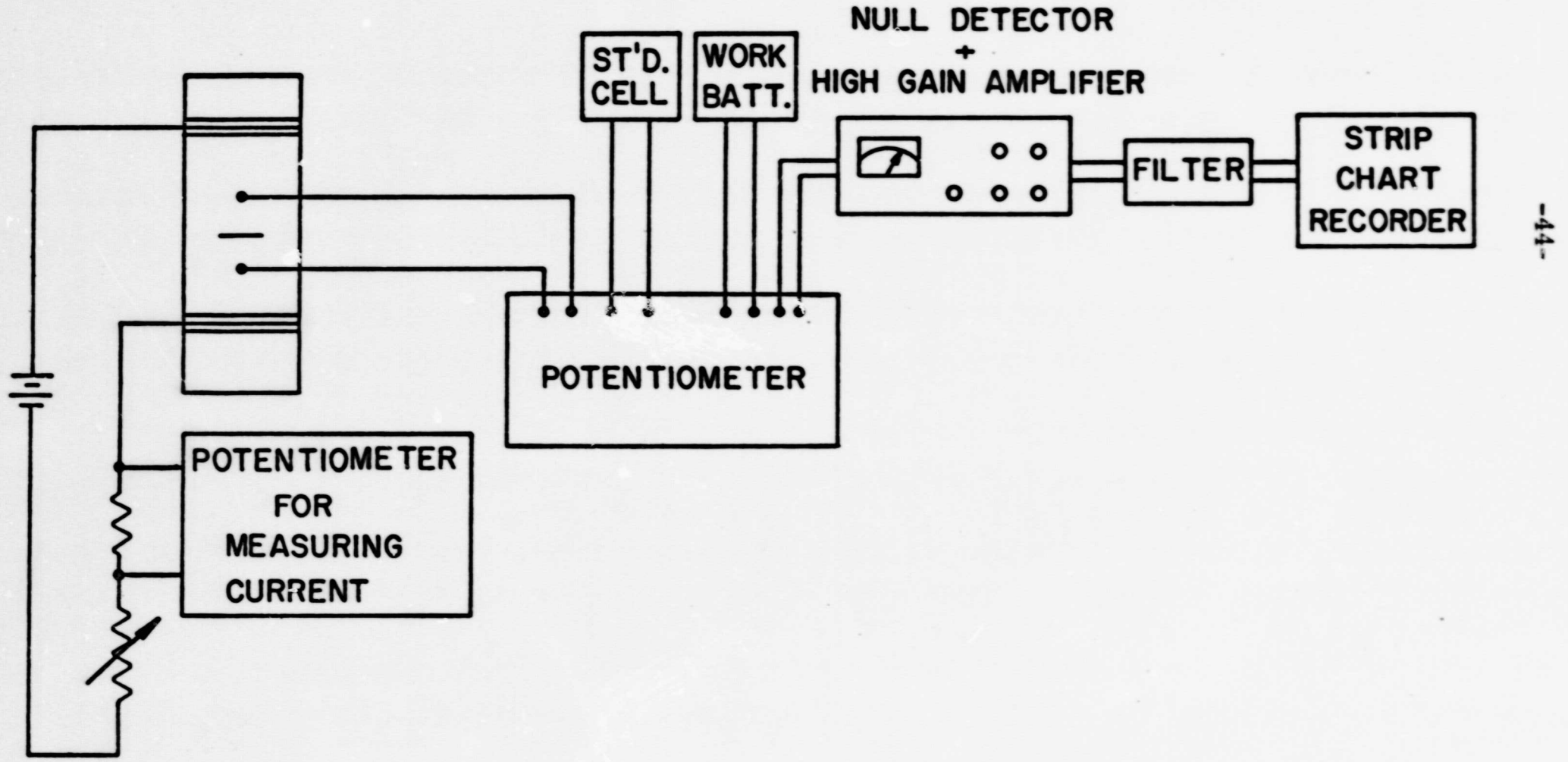

Figure 5: Schematic diagram of electrical-potential system for crack measurement

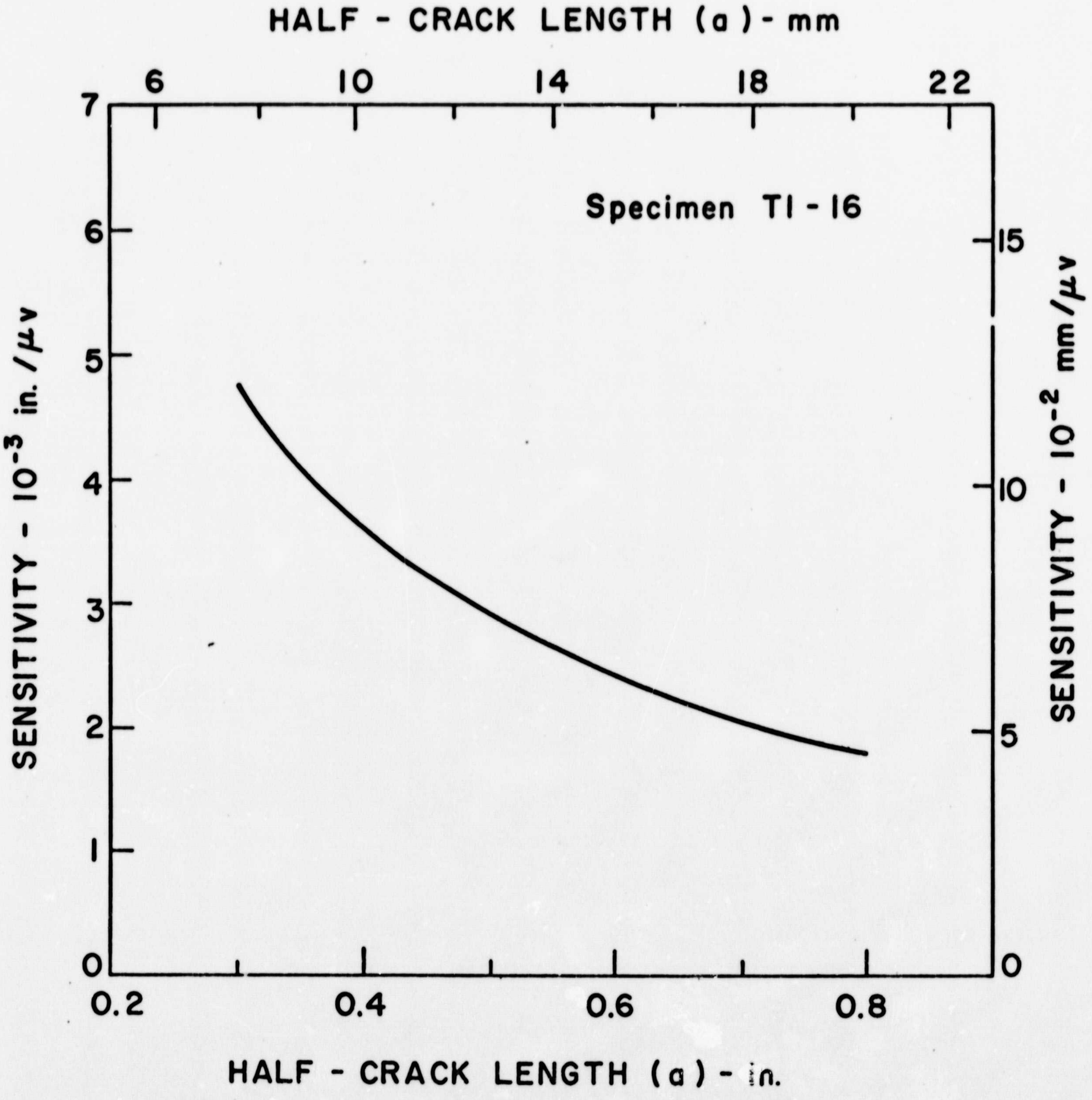

Figure 6: Variation of measurement sensitivity with crack length for a typical test specimen

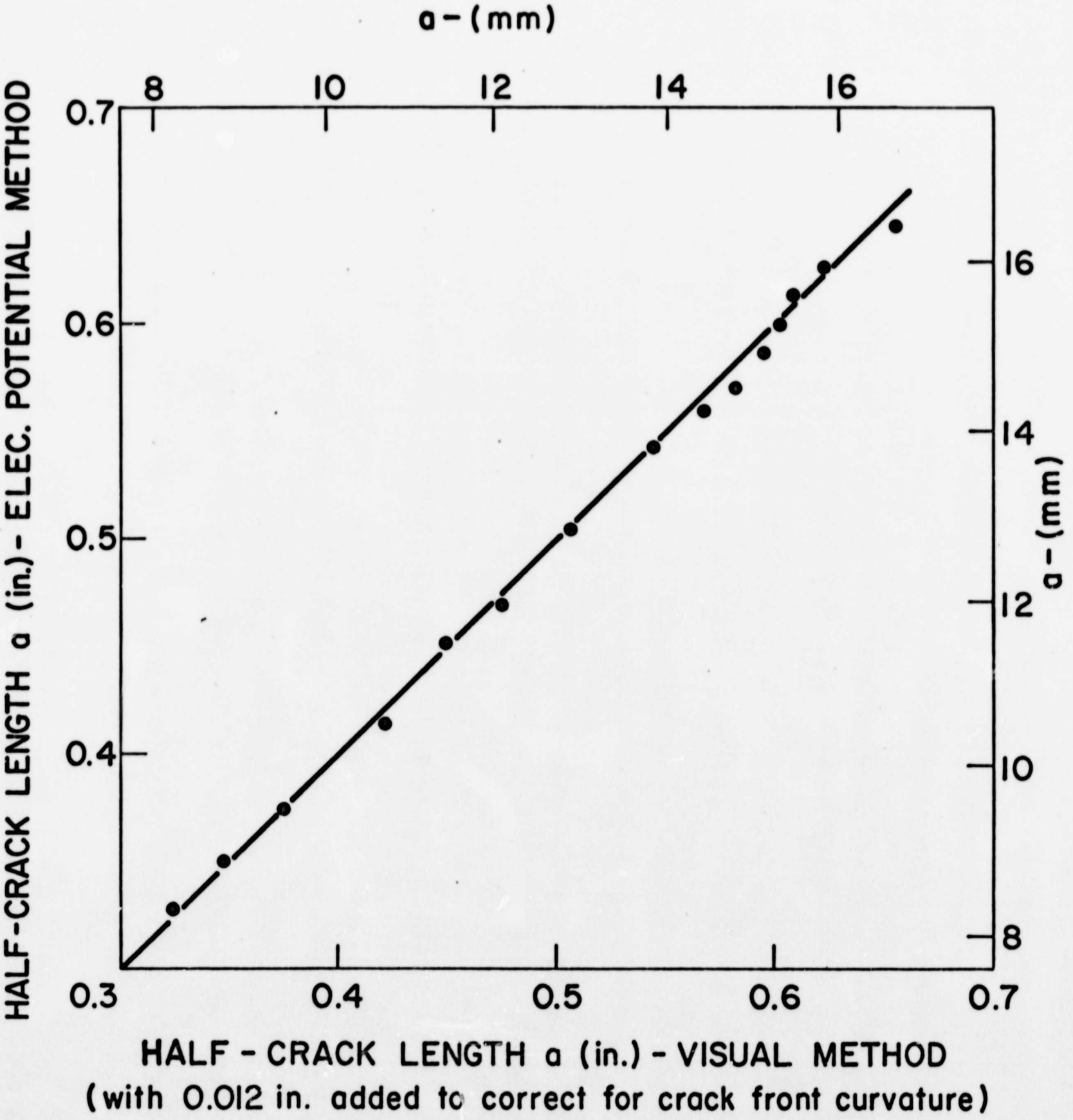

Figure 7: Correlation between crack length measurements from visual and electrical-potential methods

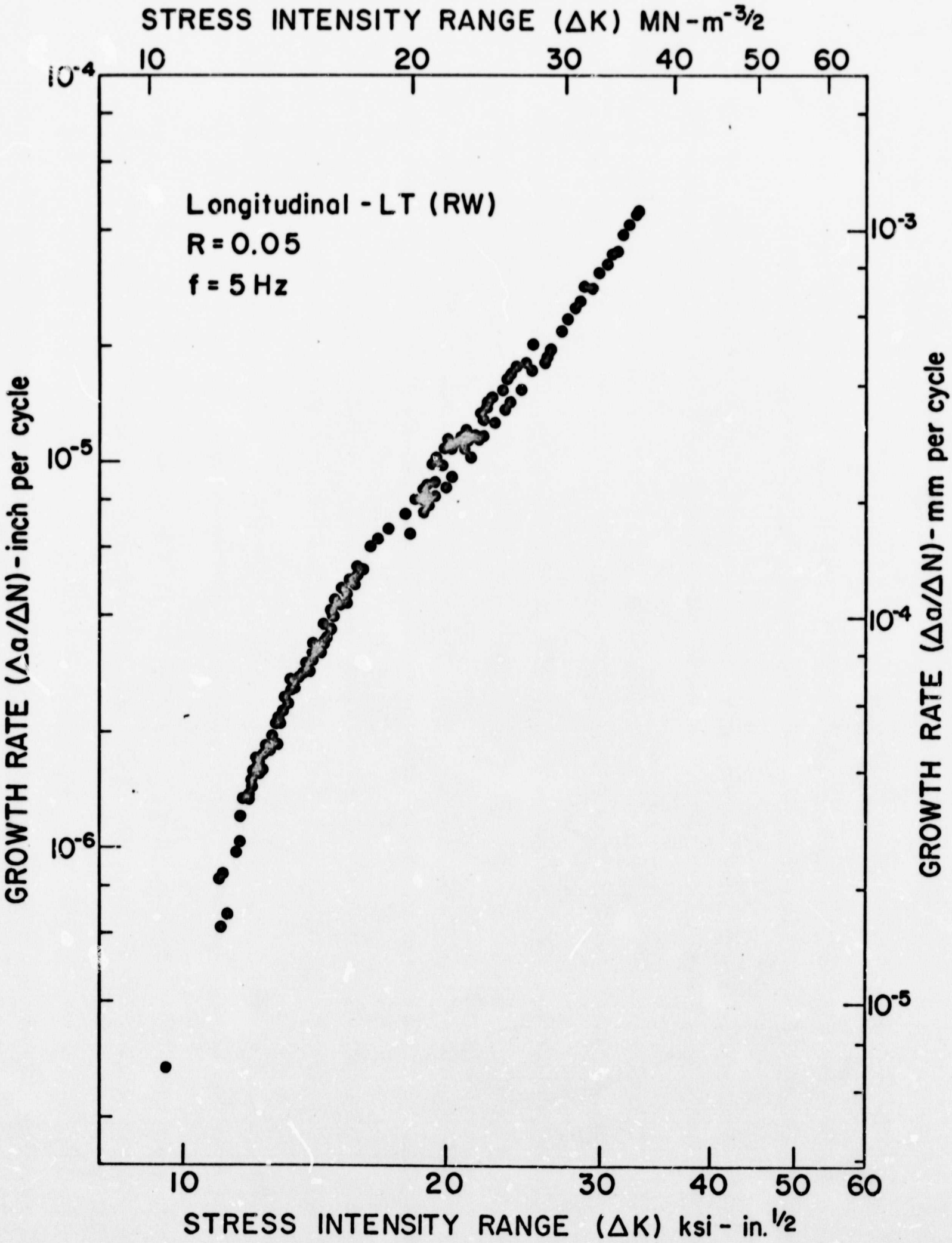

Figure 8: Rate of fatigue-crack growth in dehumidified argon at room temperature

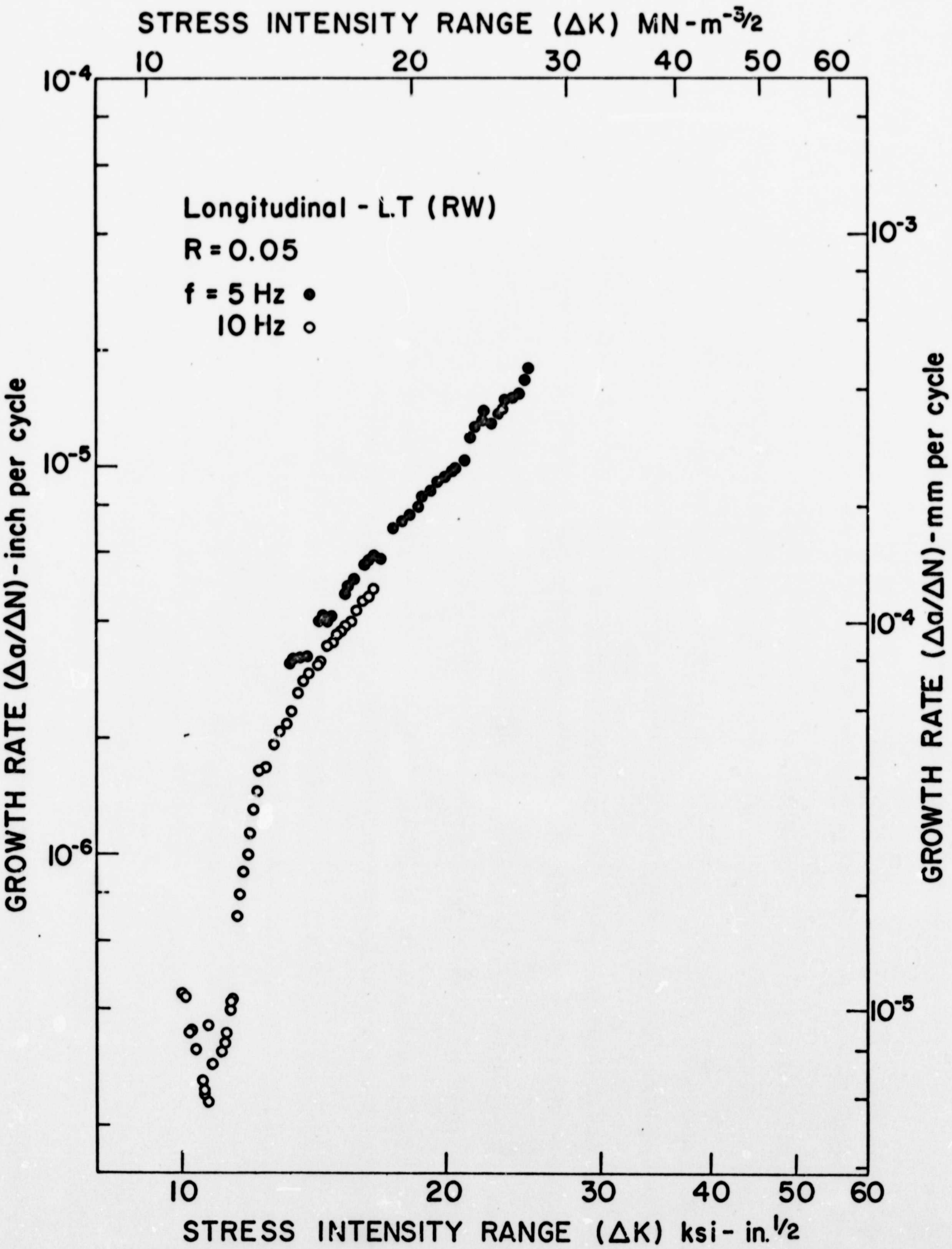

Figure 9: Rate of fatigue-crack growth in dehumidified argon at 49°C.

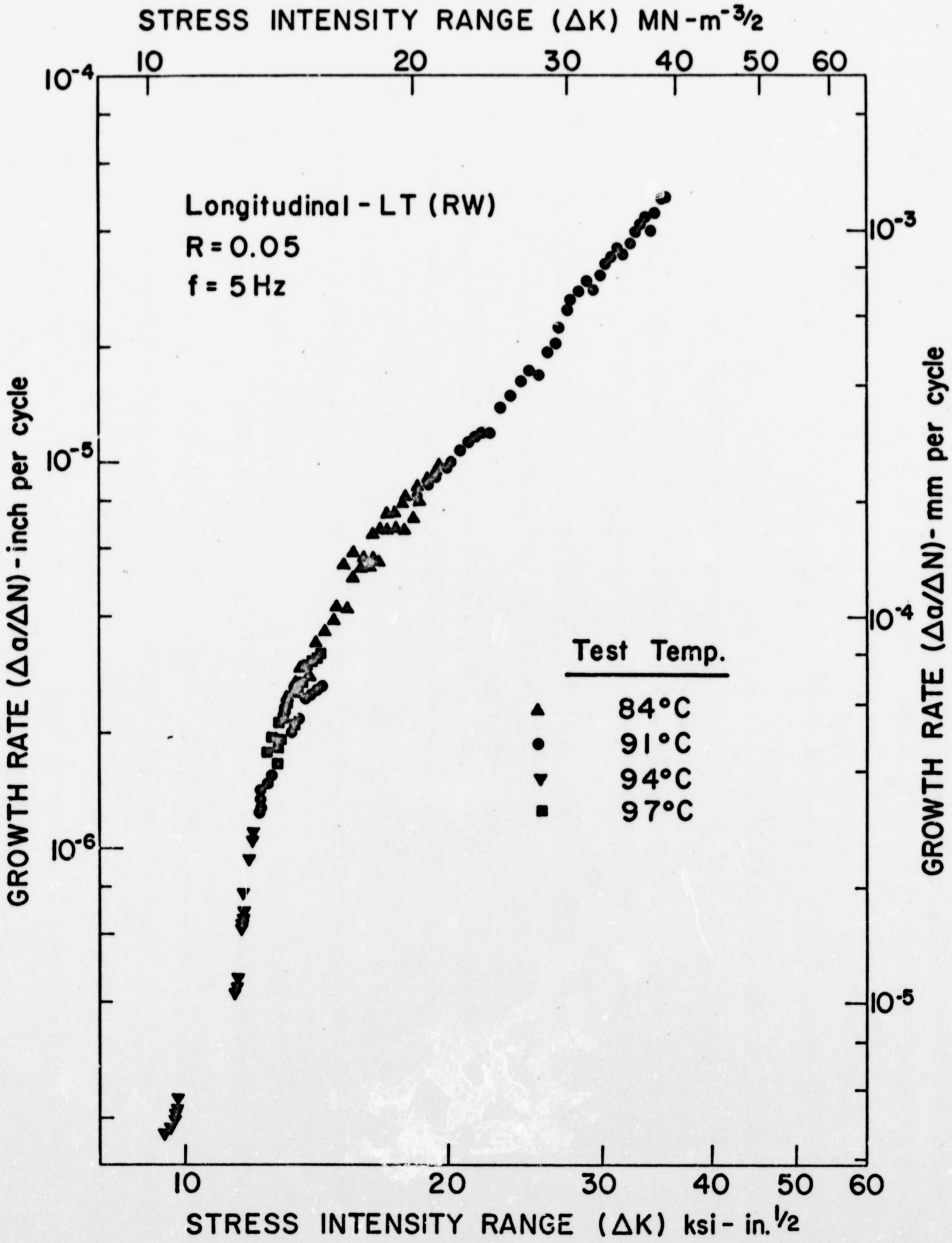

Figure 10: Rate of fatigue-crack growth in dehumidified argon at 80° to 100°C.

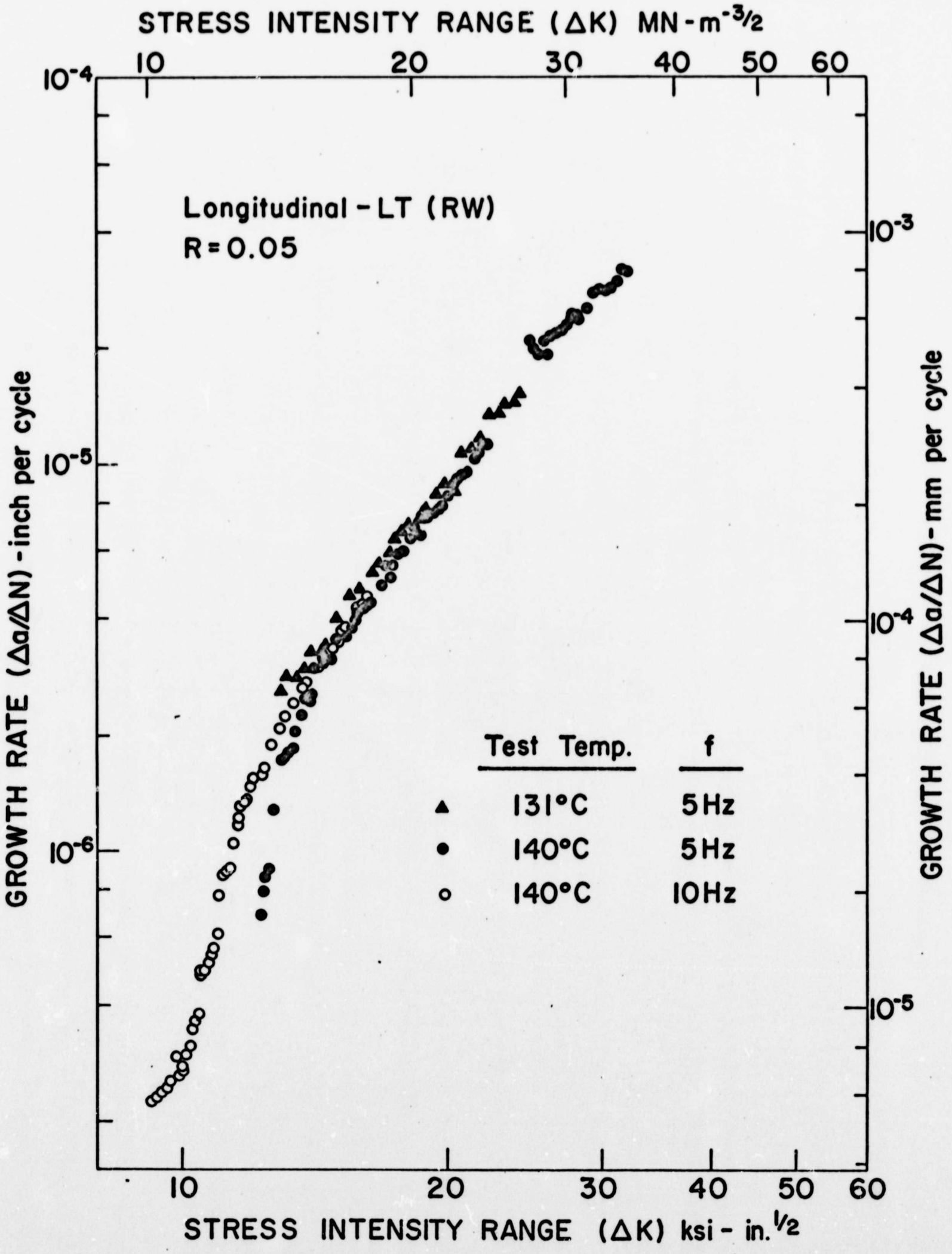

Figure 11: Rate of fatigue-crack growth in dehumidified argon at 130° to 140°C.

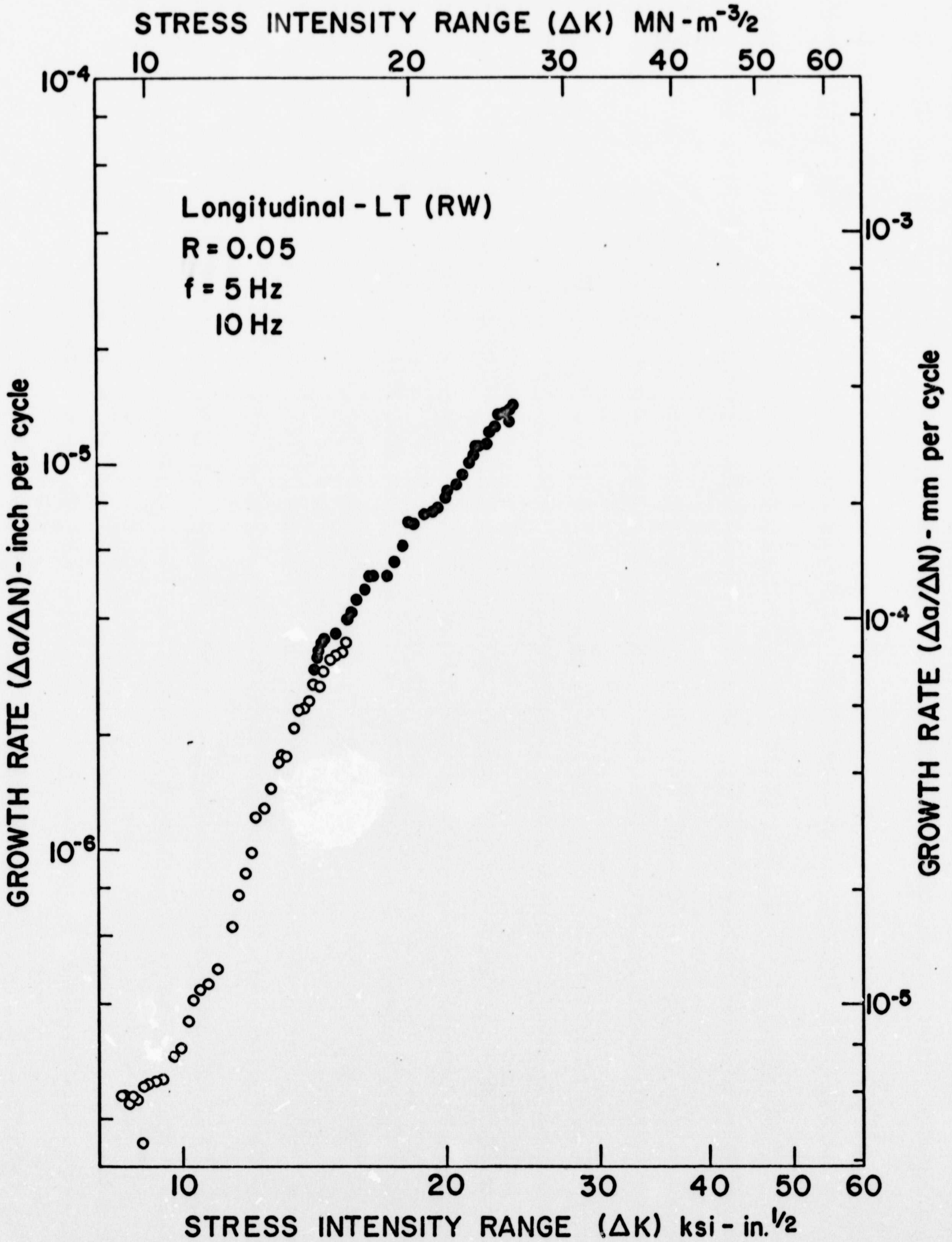

Figure 12: Rate of fatigue-crack growth in dehumidified argon at 200° to 210°C.

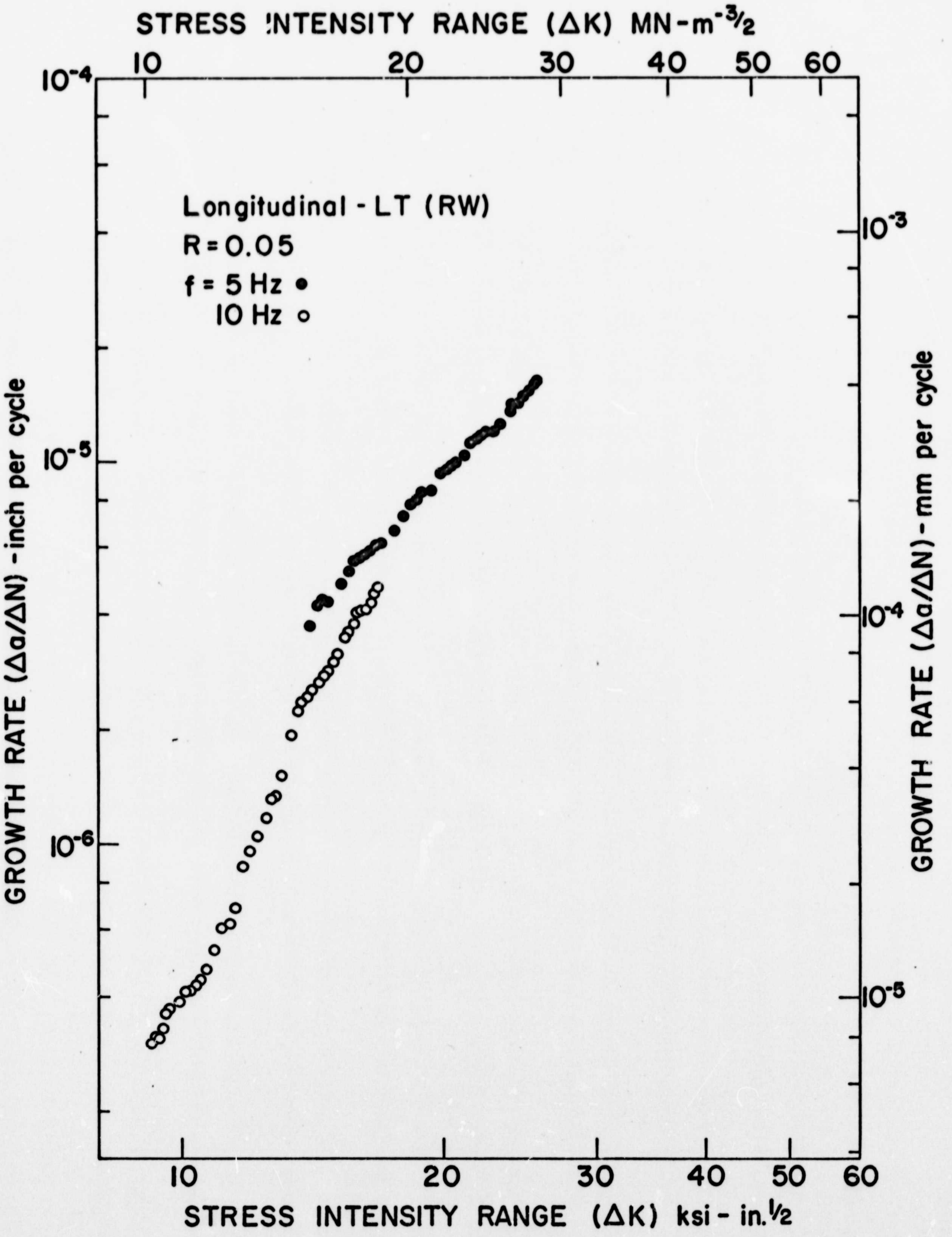

Figure 13: Rate of fatigue-crack growth in dehumidified argon at 290°C

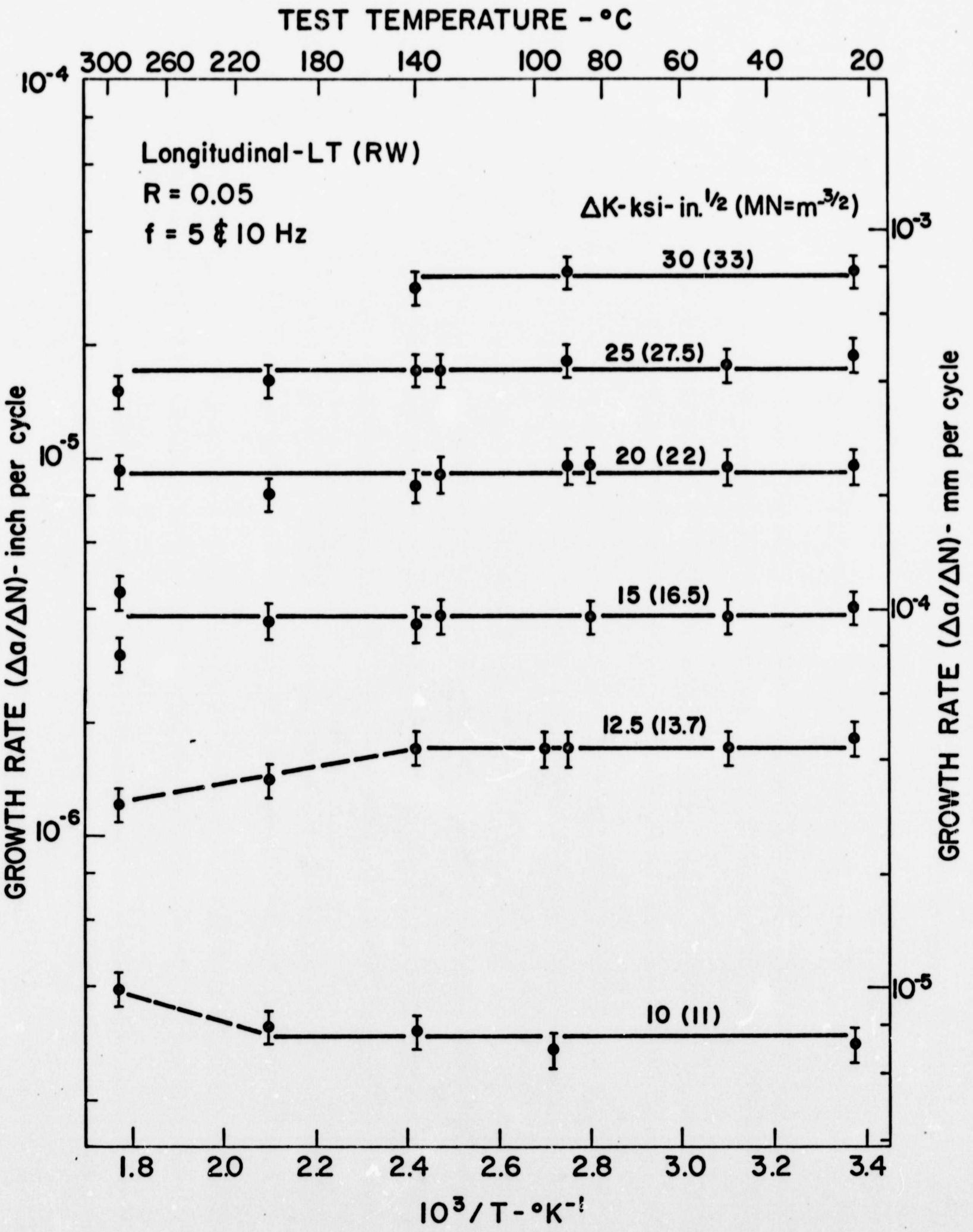

Figure 14: Influence of temperature on fatigue-crack growth in dehumidified argon at various K levels

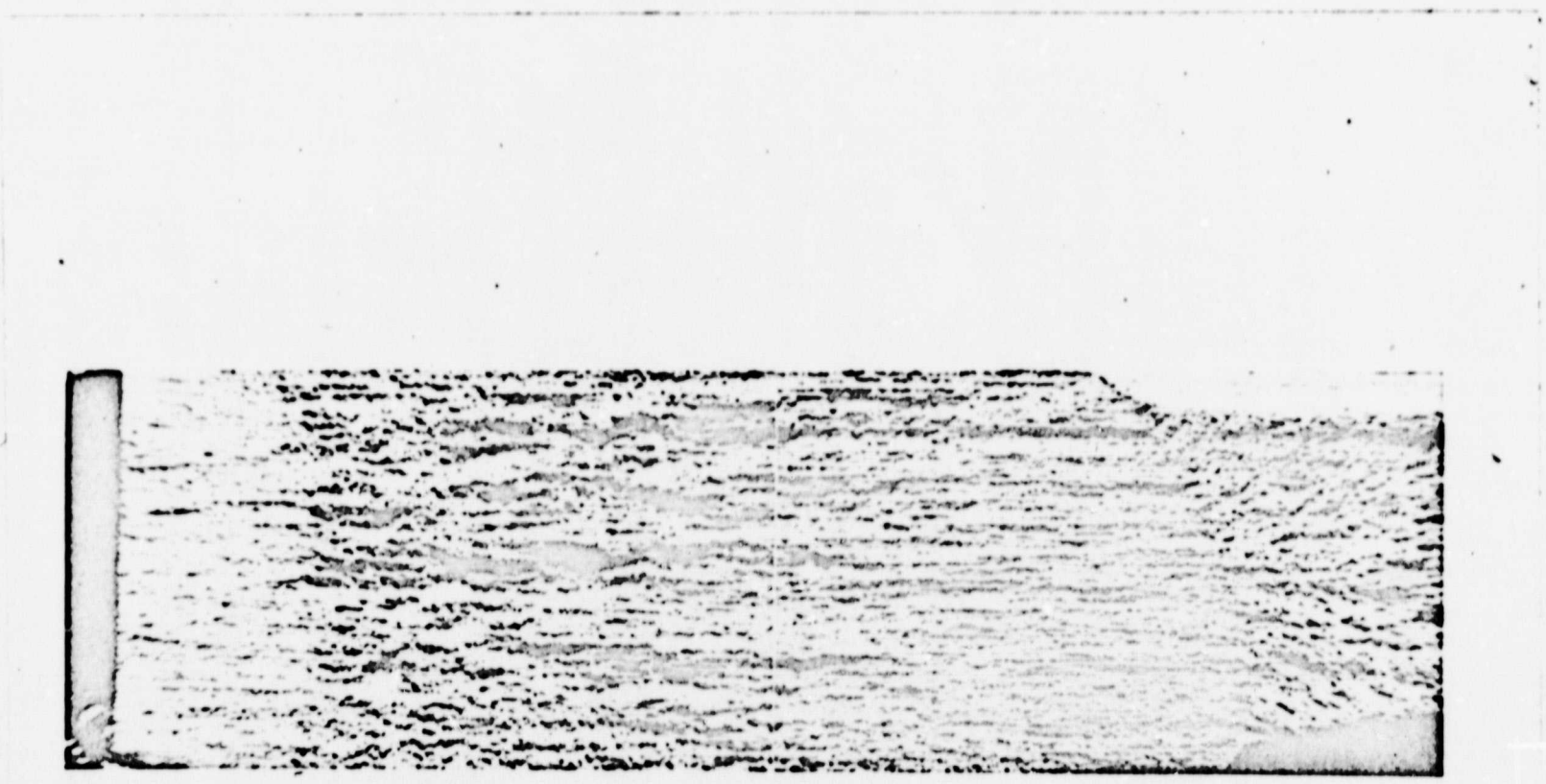

Figure 15: Optical macro-fractograph showing transition from "coarse" to "fine" mode of fracture.(Specimen tested at 300 to 6000 lbs. at 10 Hz. after fatigue precrack. Regions shown are, from left to right, fatigue precrack, coarse region, fine region, and tensile failure.)

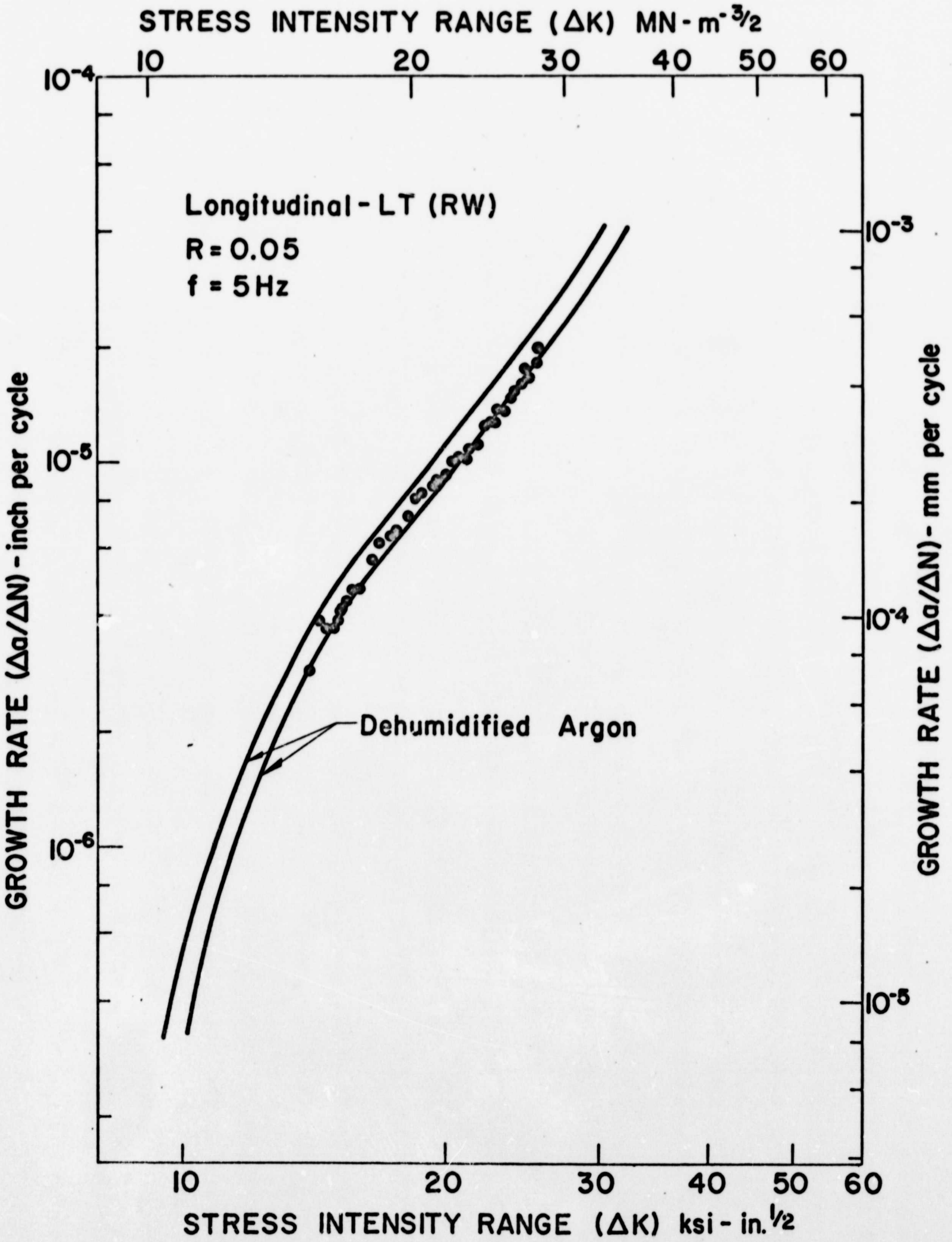

Figure 16: Rate of fatigue-crack growth in dehumidified oxygen at room temperature

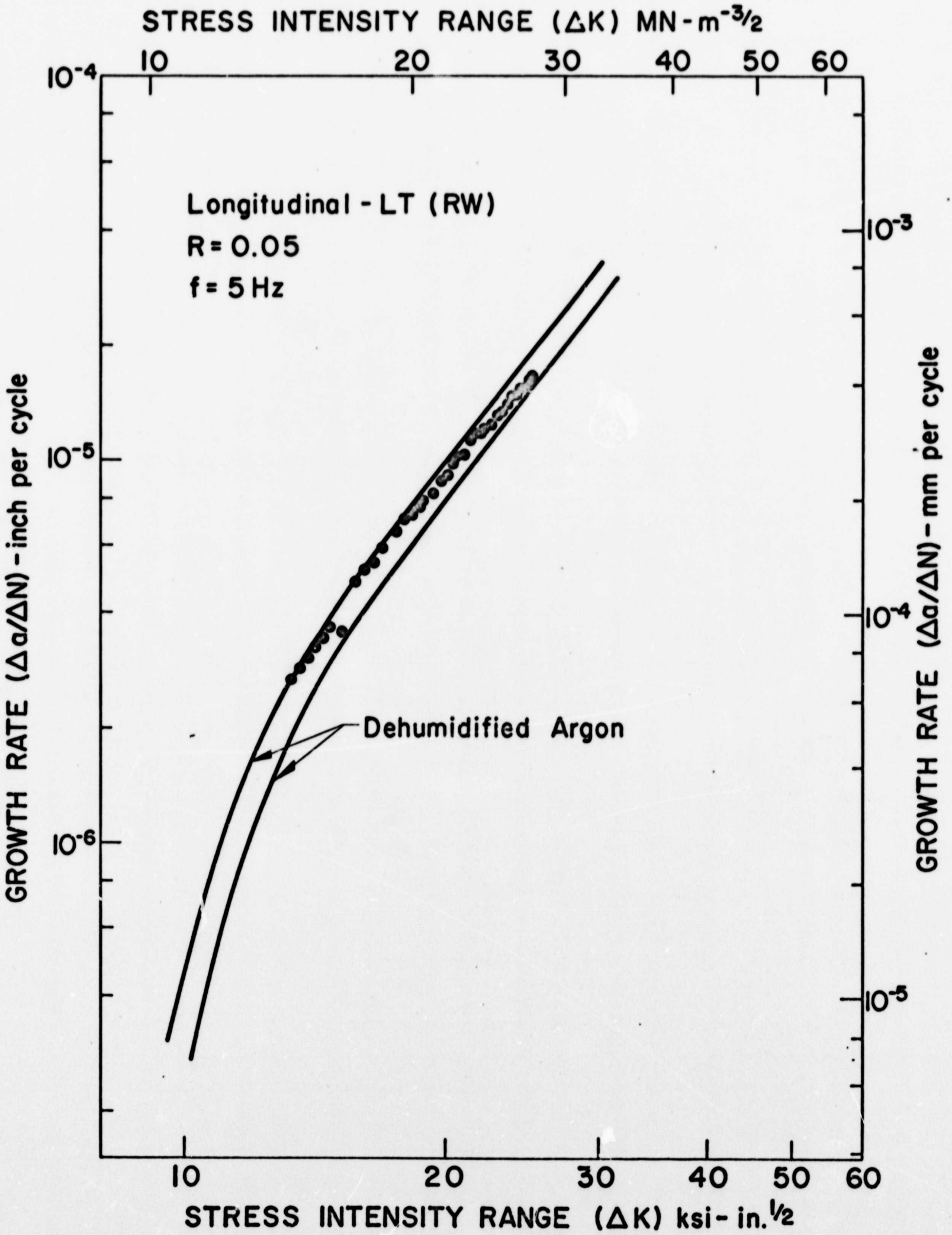

Figure 17: Rate of fatigue-crack growth in dehumidified oxygen at 130°C

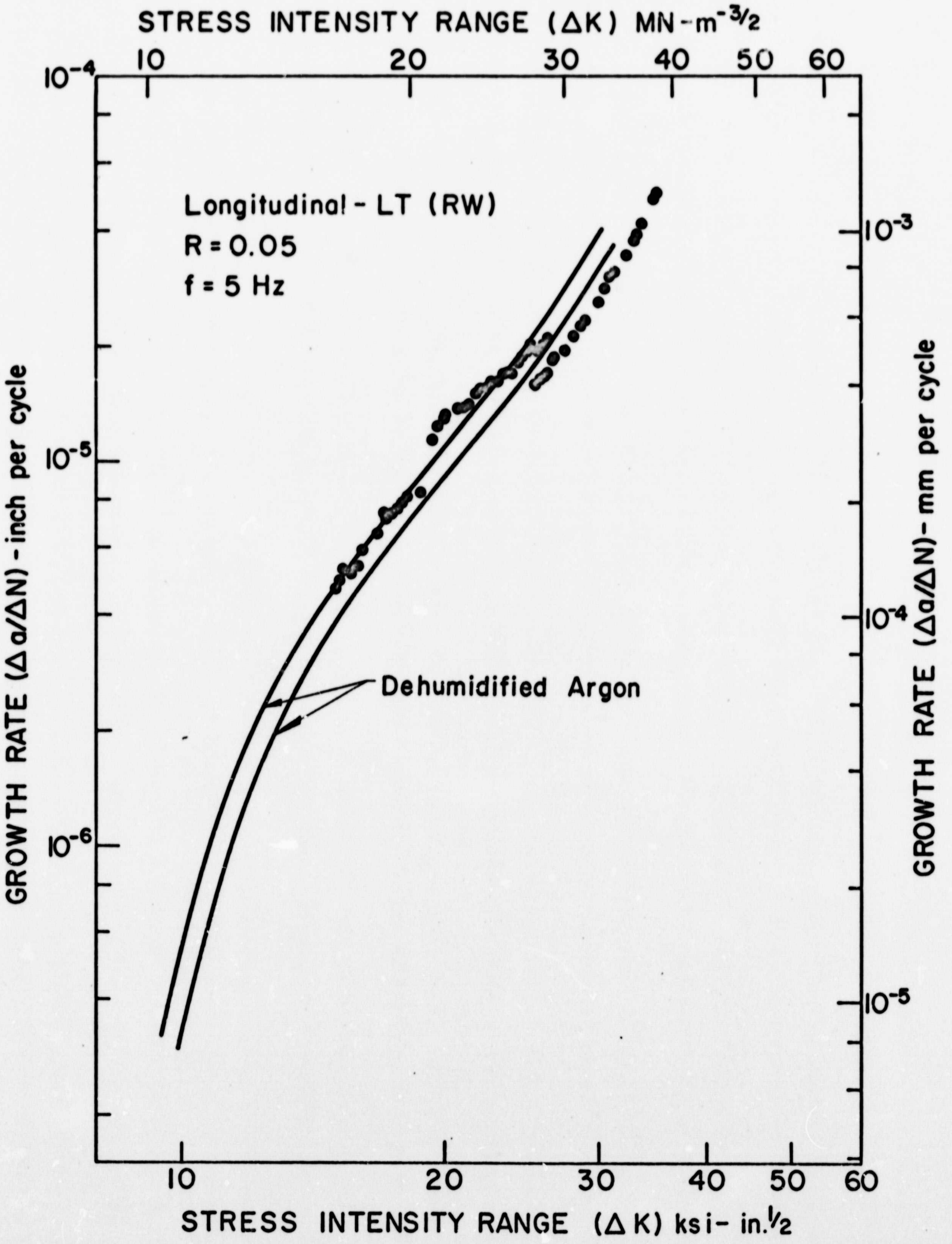

Figure 18: Rate of fatigue-crack growth in dehumidified hydrogen at room temperature

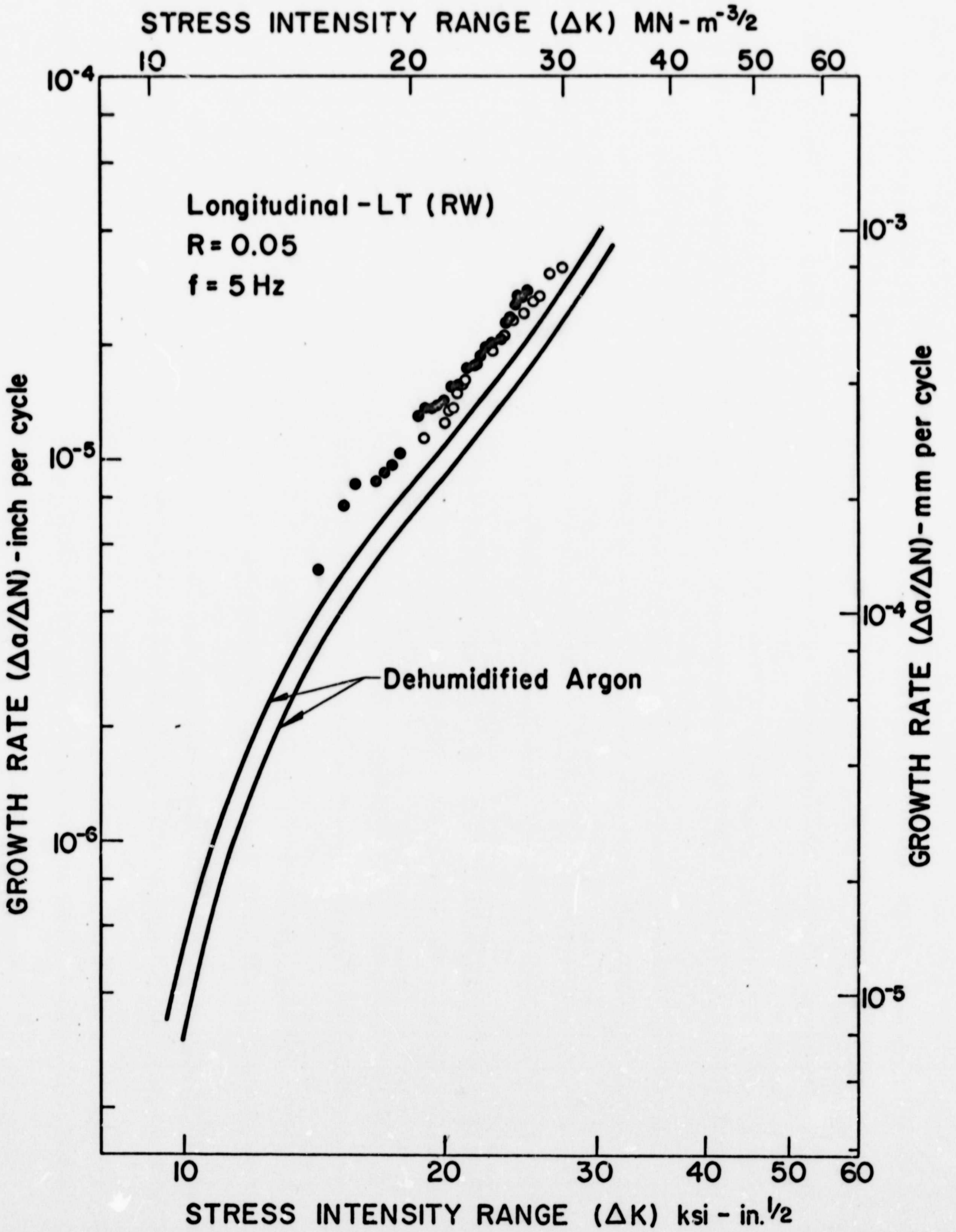

Figure 19: Rate of fatigue-crack growth in distilled water at room temperature

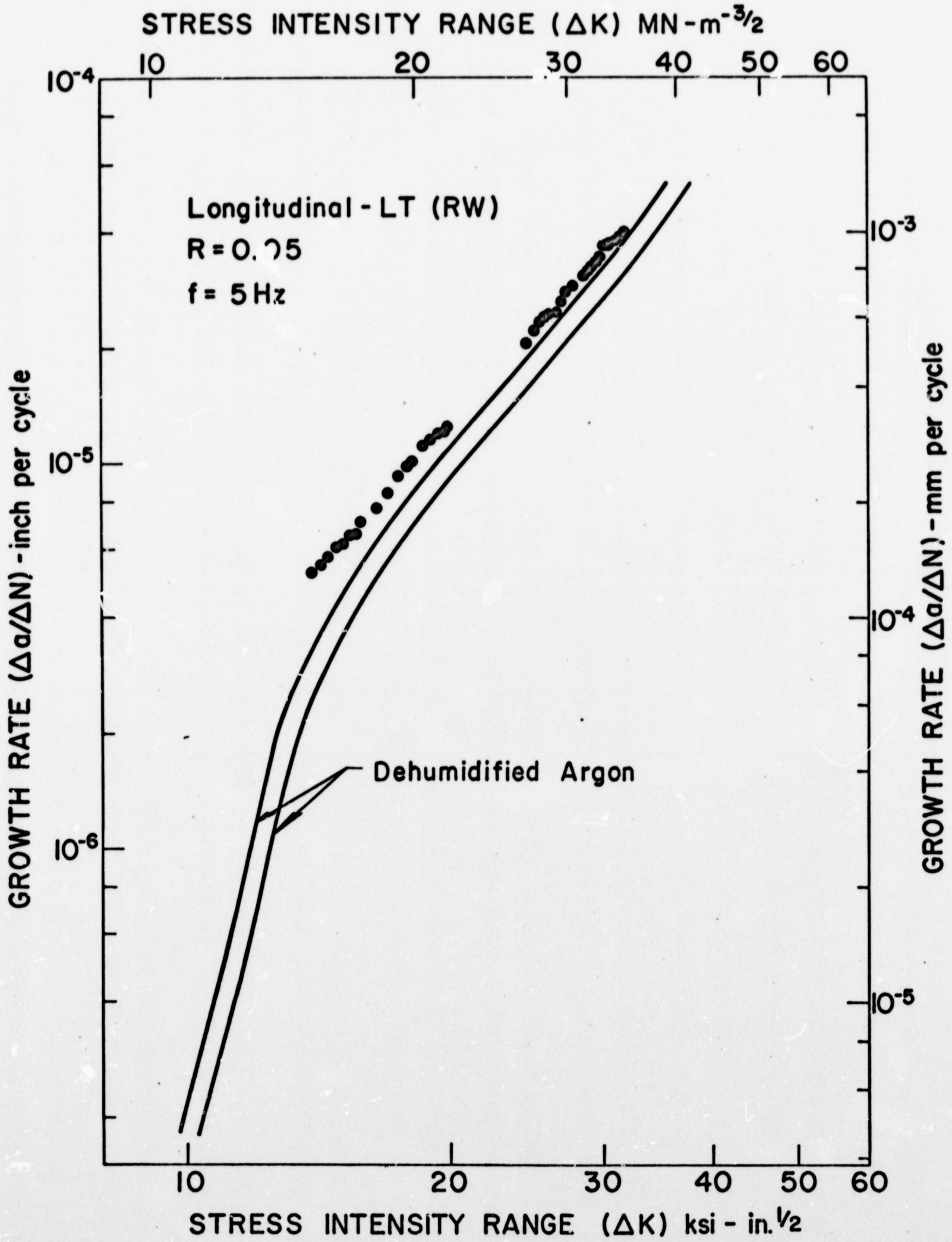

Figure 20: Rate of fatigue-crack growth in distilled water at 85°C

2-2

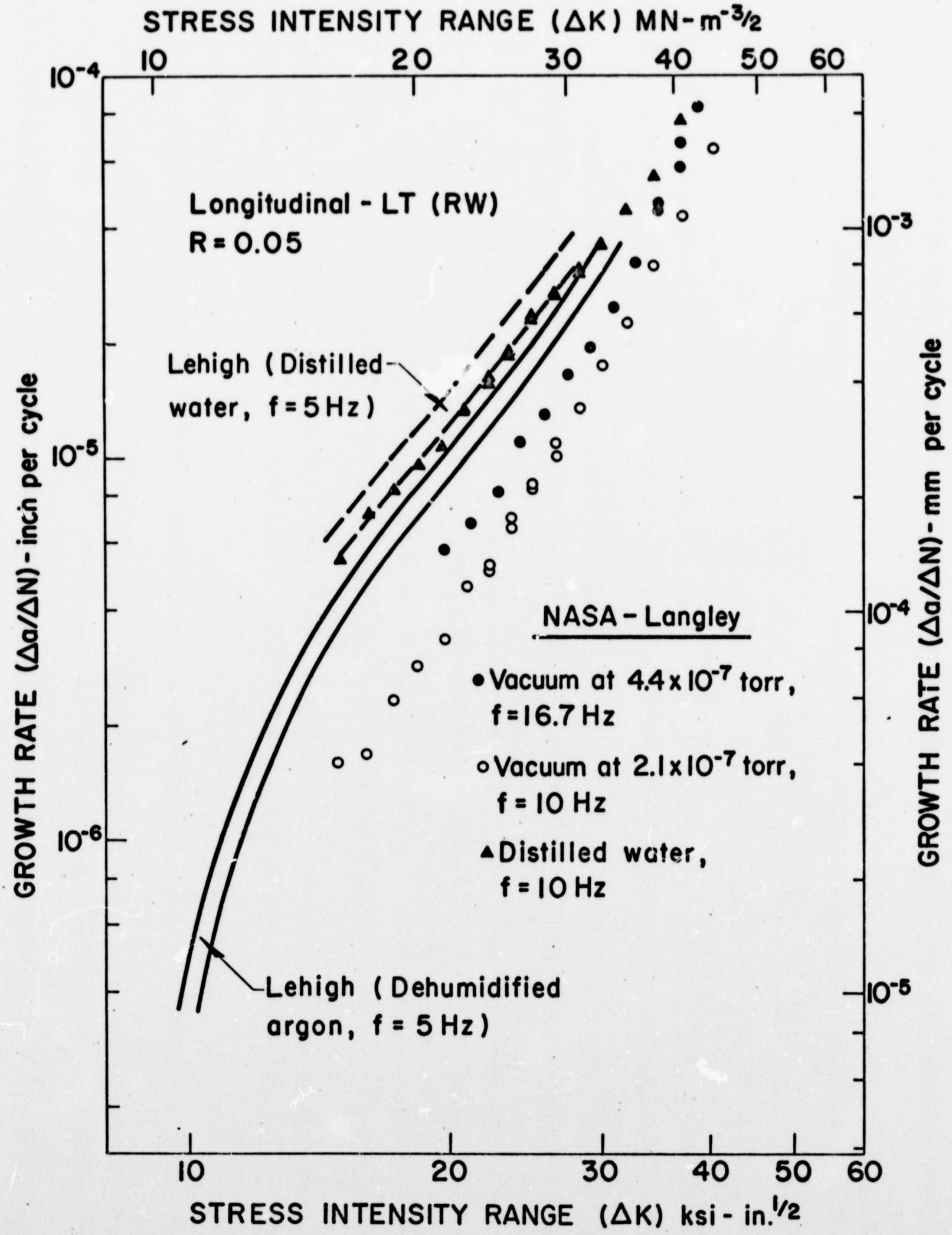

Figure 21: Comparison of NASA and Lehigh test results in vacuum, dehumidified argon and distilled water at room temperature

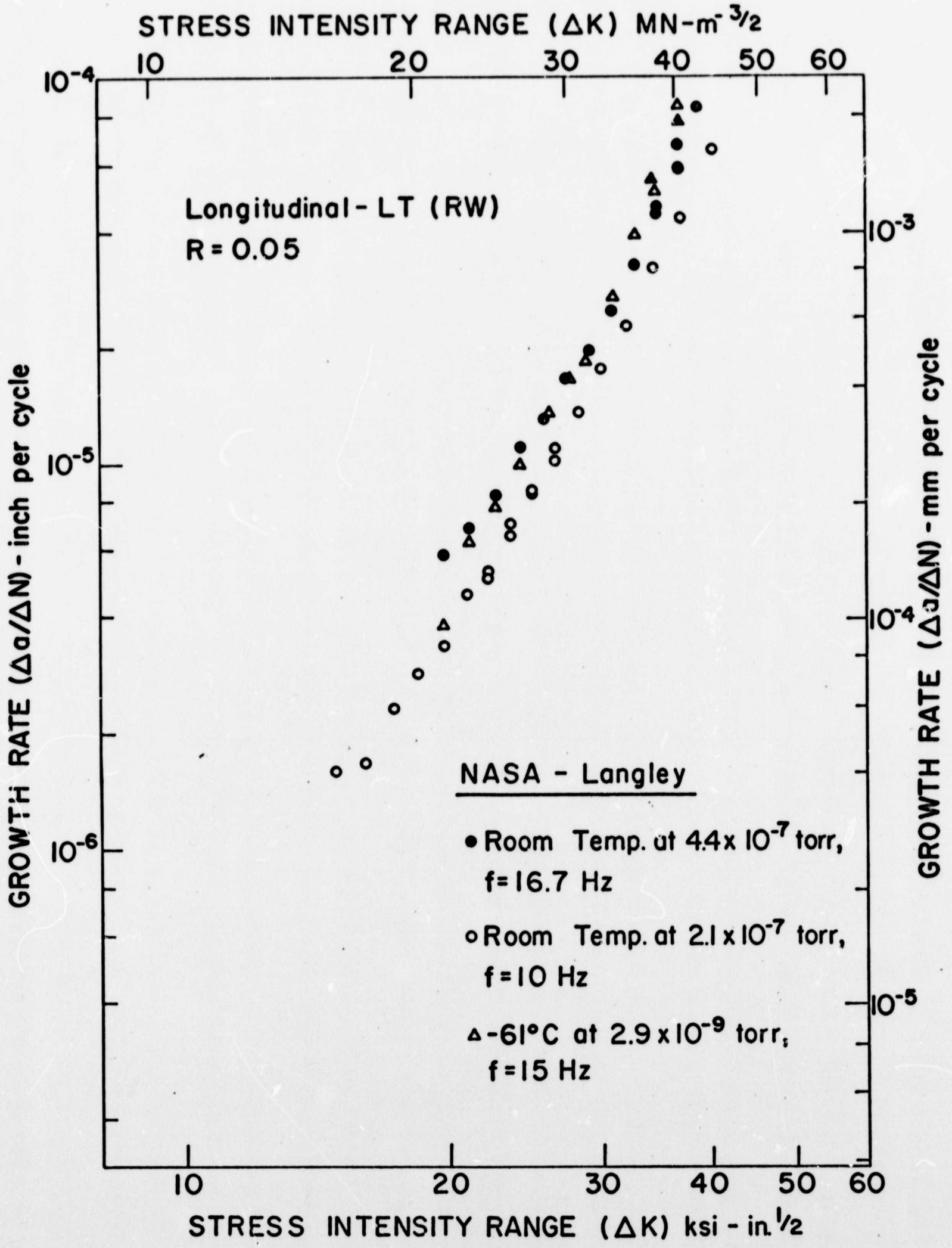

Figure 22: Rate of fatigue-crack growth in vacuum at room temperature and -61°C

(a) Argon at RT T1-24

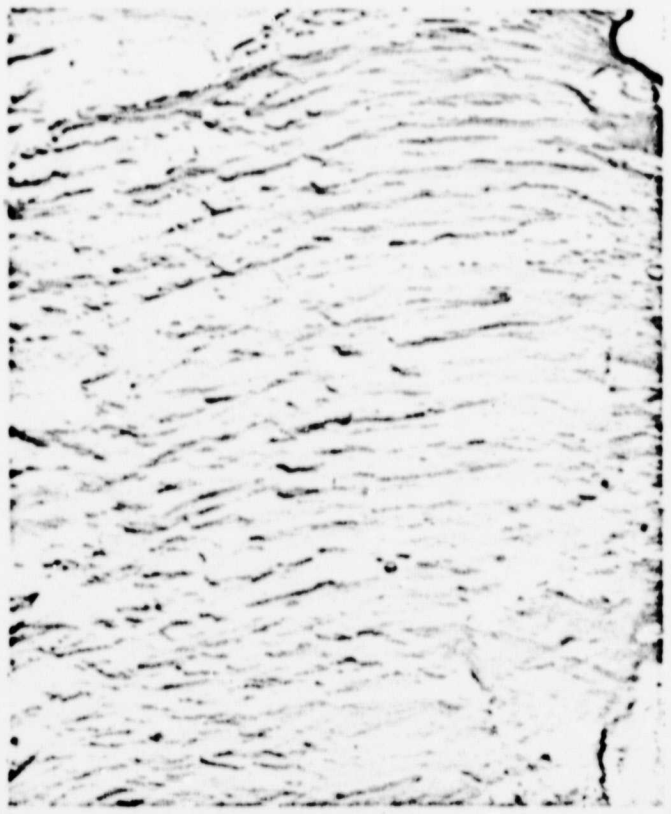

(b) Argon at 130°C T1-18

(c) Vacuum (4.4×10^{-7} torr) T1-25 at RT

(d) Vacuum (2.9×10^{-9} torr) T1-26 at -61°C

Figure 23: Typical electron-micrographs of fatigue fracture surfaces of specimens tested in the various environments and temperatures (5700X)

(e) Distilled water at RT T1-23

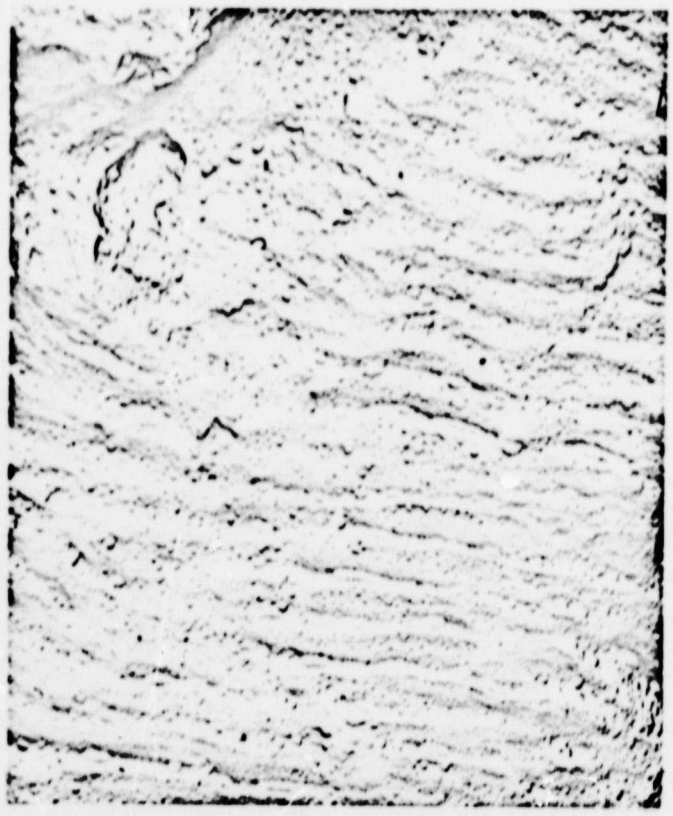

(f) Hydrogen at RT T1-17

Figure 23 (continued): Typical electron-micrographs of fatigue fracture surfaces of specimens tested in the various environments and temperatures (5700X)

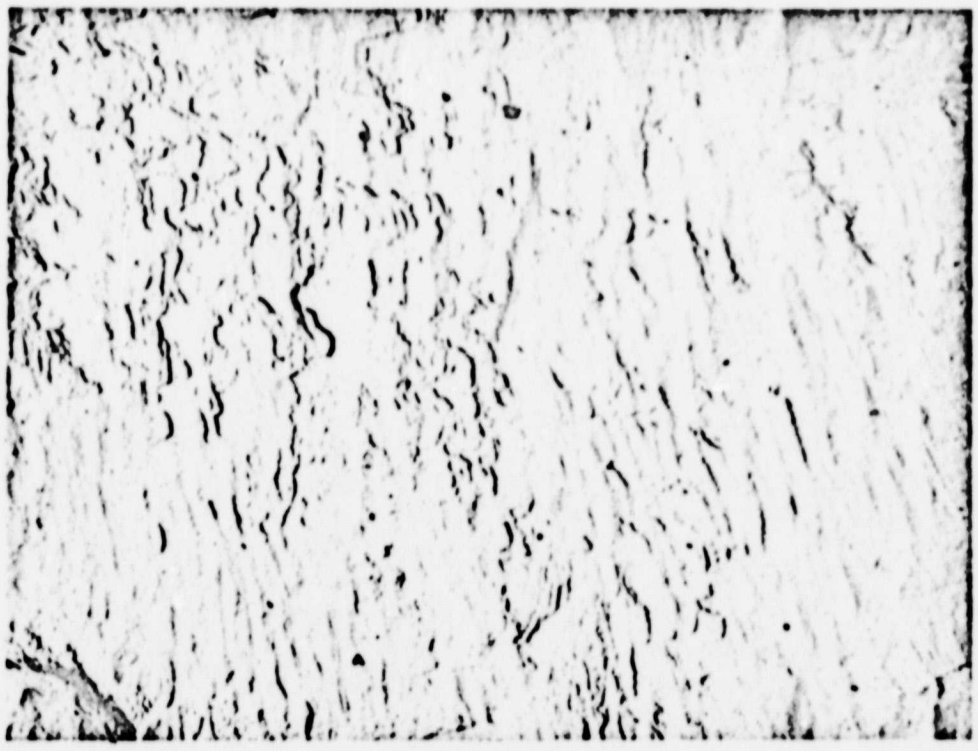

(a) 0° tilt

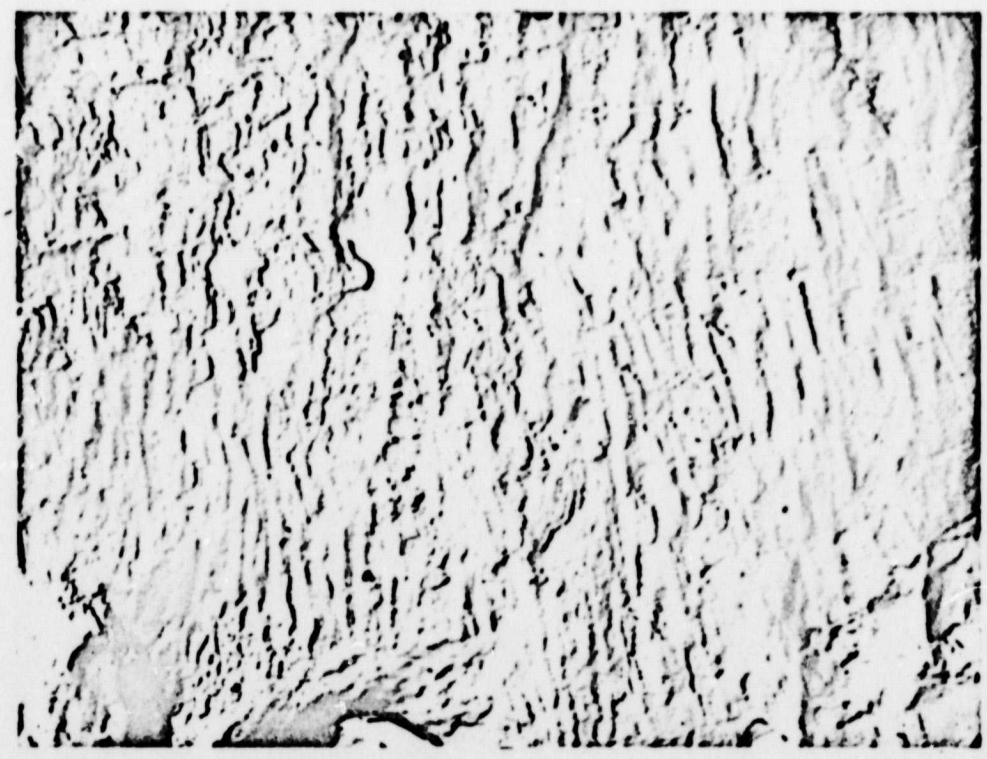

(b) 30° tilt

Specimen T1-25

Figure 24: Effect of replica tilt angle on fractographic appearance (~7300X)

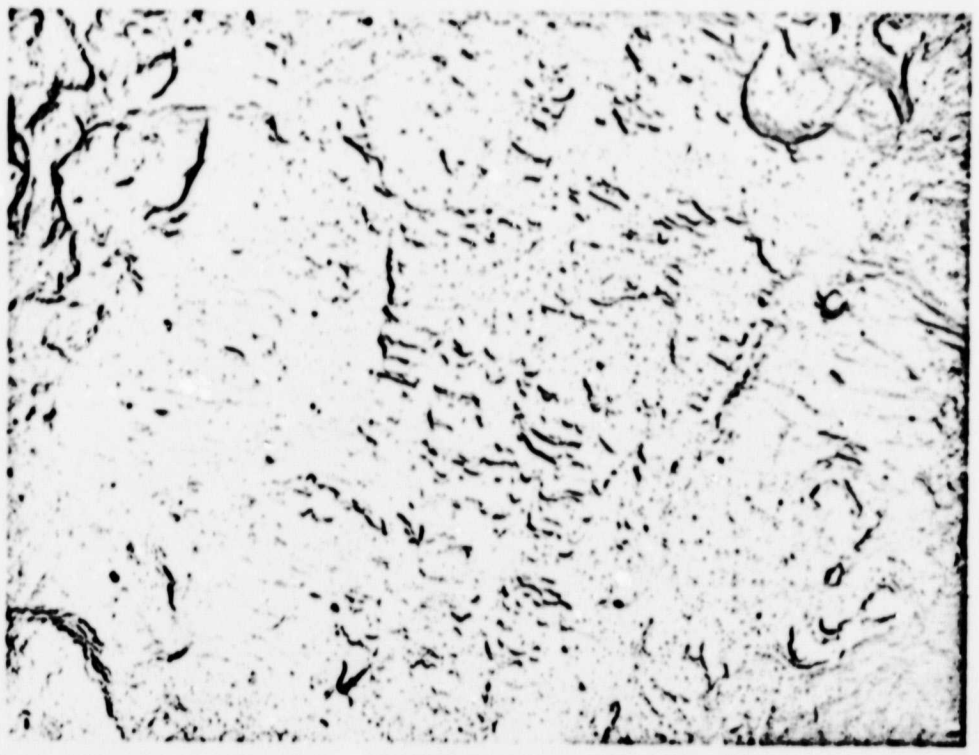

(a) -15° tilt

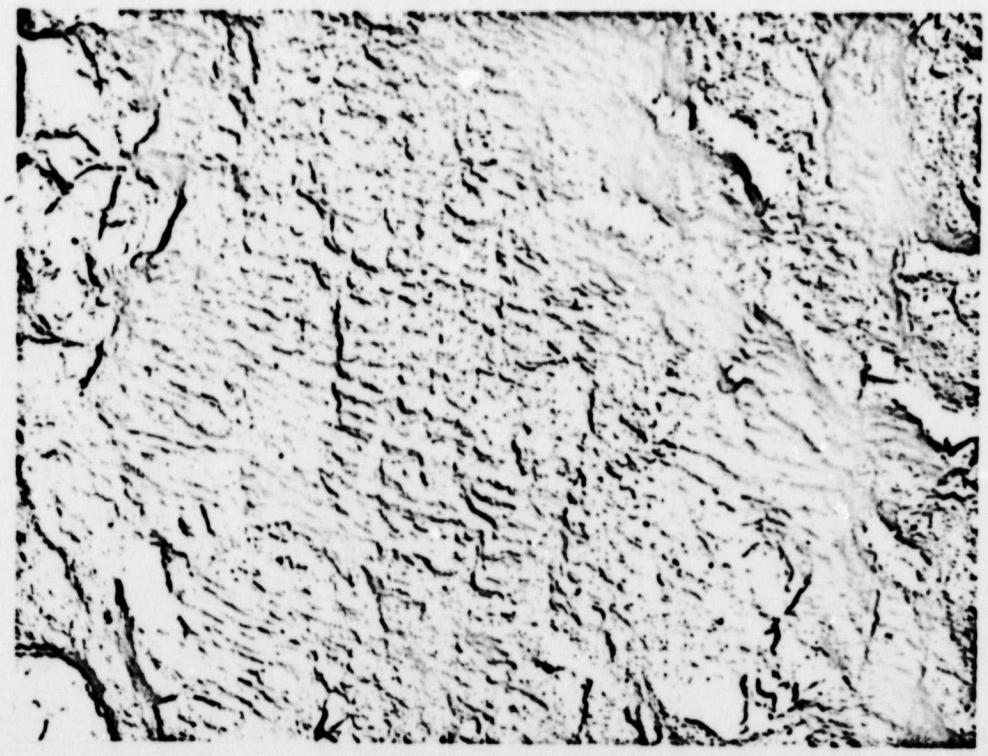

(b) +30° tilt

Specimen T1-25

Figure 25: Effect of replica tilt angle on fractographic appearance (~5300X)

(a) "Fine" region 7100X

(b) "Coarse" region 3200X

Specimen T1-30

Figure 26: Typical electron-micrographs of fatigue fracture surfaces in the "coarse" and "fine" regions

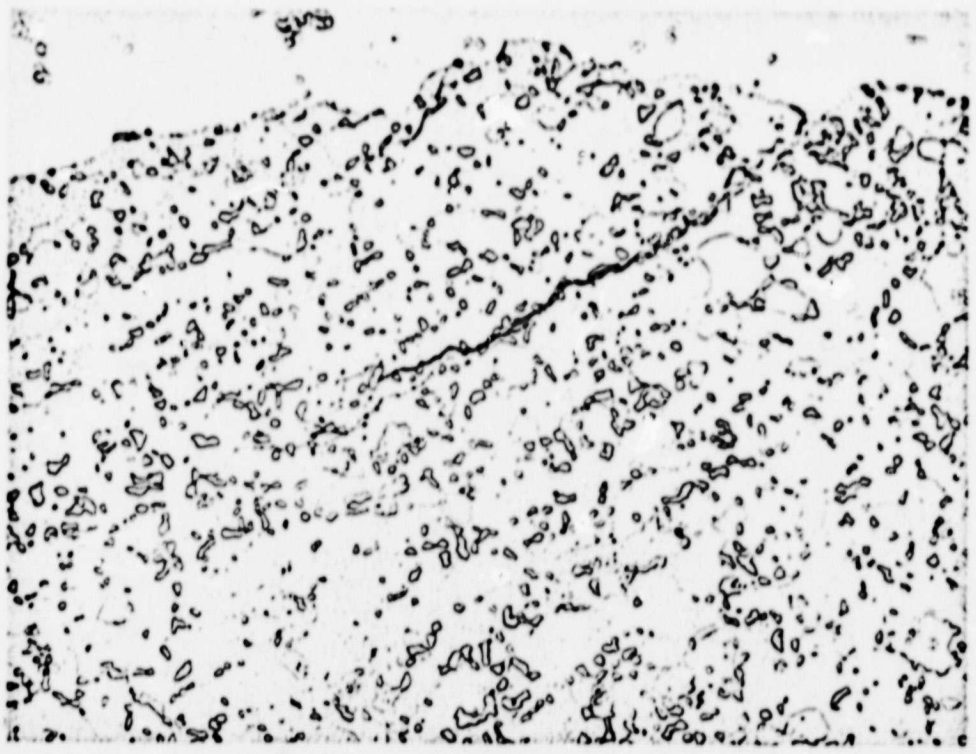

(a) 530X

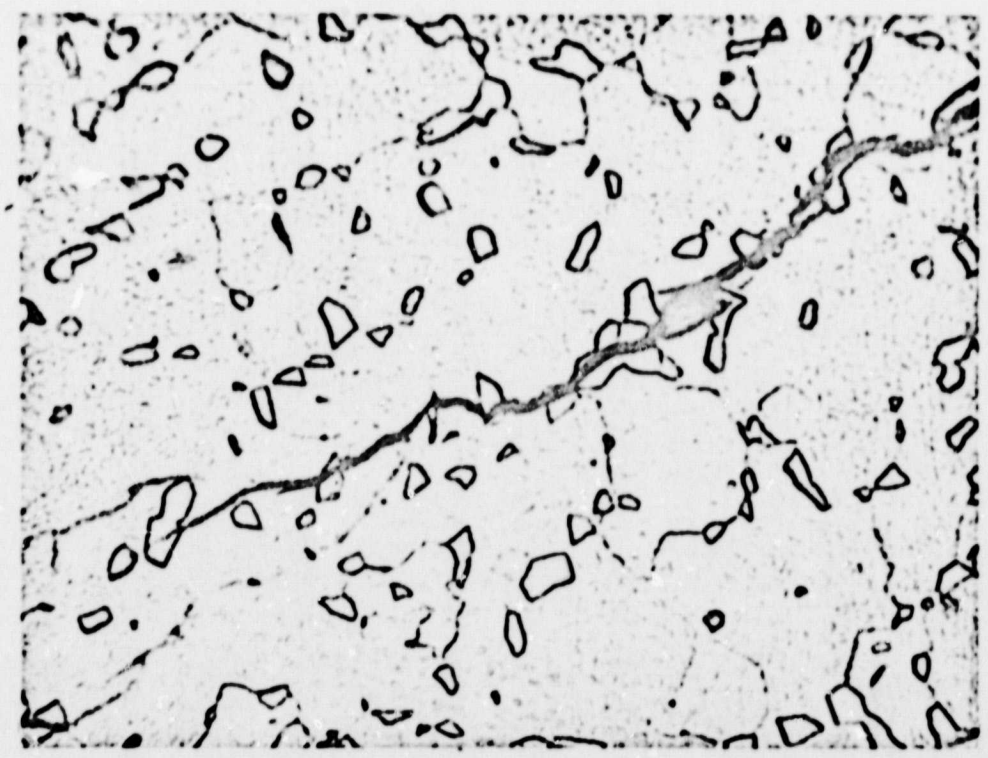

(b) 1200X

Specimen T1-11

Figure 27: Optical micrographs of branching cracks in the "coarse" region

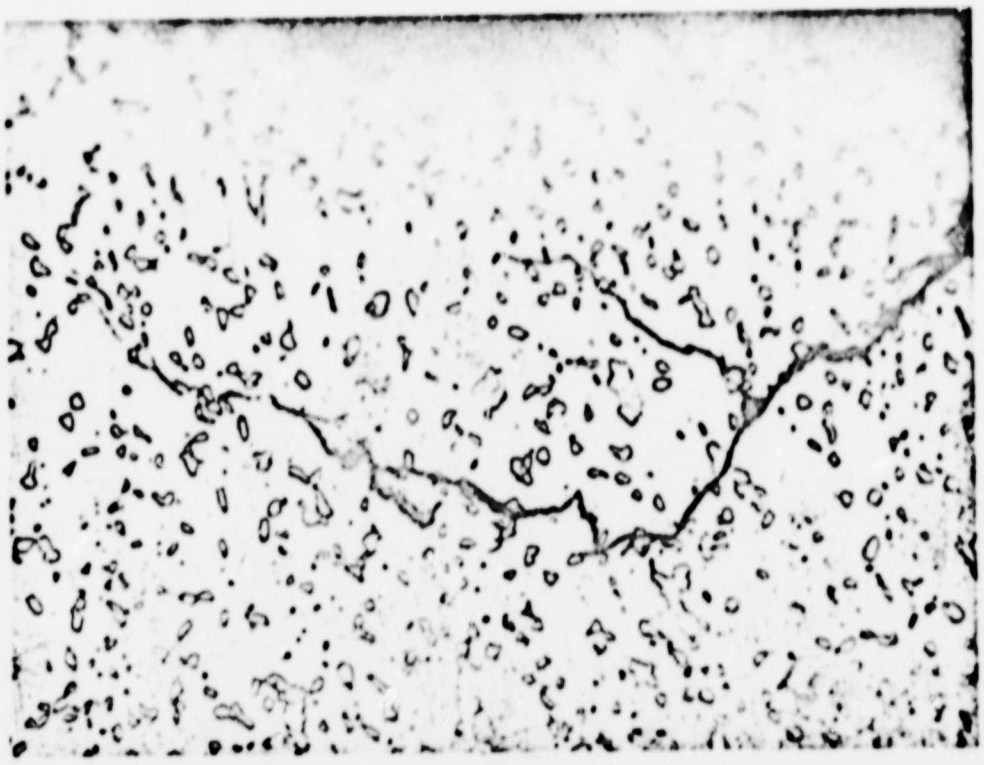

(a) 930X

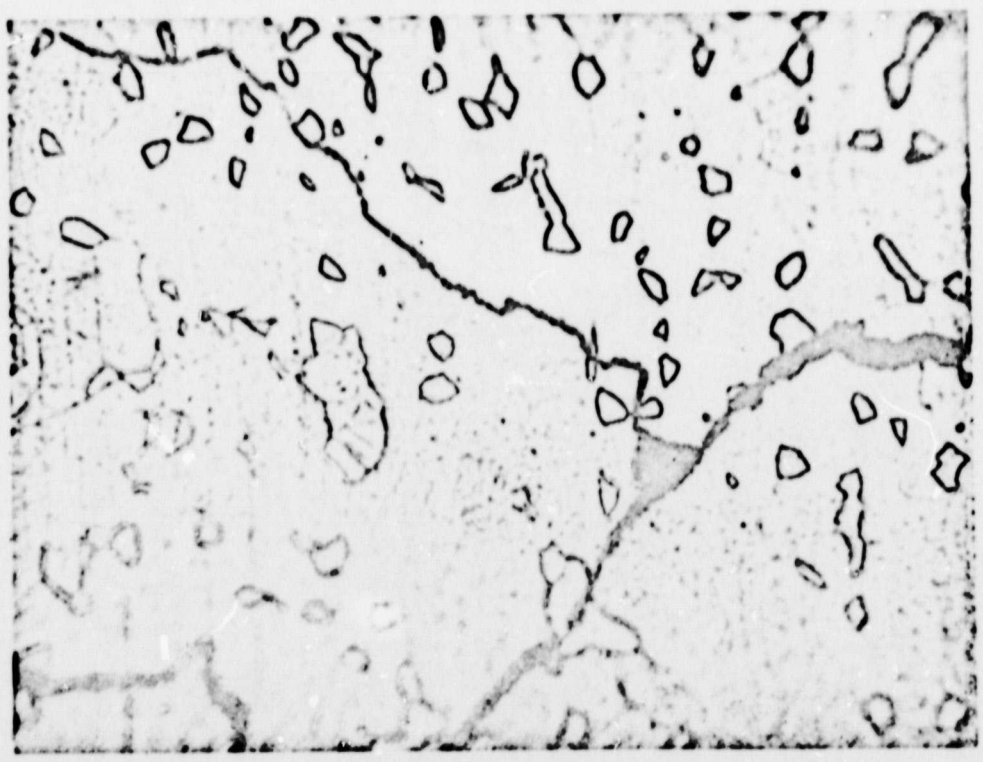

(b) 1200X

Specimen T1-11

Figure 28: Optical micrographs of branching cracks in the "coarse" region